AD_____
(Leave blank)

Award Number:
W81XWH-06-1-0229

TITLE:
Investigating the Functional Role of Prostate-Specific Membrane Antigen and Its Enzymatic Activity in Prostate Cancer Metastasis

PRINCIPAL INVESTIGATOR:
Sharron X. Lin, Ph.D.

CONTRACTING ORGANIZATION:
The General Hospital Corporation
Boston, M 02114-2698

REPORT DATE:
November 2009

TYPE OF REPORT:
Final

PREPARED FOR: U.S. Army Medical Research and Materiel Command
Fort Detrick, Maryland 21702-5012

DISTRIBUTION STATEMENT: (Check one)

X Approved for public release; distribution unlimited

Distribution limited to U.S. Government agencies only; report contains proprietary information

REPORT DOCUMENTATION PAGE

Form Approved
OMB No. 0704-0188

1. REPORT DATE *(DD-MM-YYYY)*	2. REPORT TYPE	3. DATES COVERED *(From - To)*
28/11/09	Final	JAN 2006 - 28 OCT 2009

4. TITLE AND SUBTITLE

Investigating the Functional Role of Prostate-Specific Membrane Antigen and Its Enzymatic Activity in Prostate Cancer Metastasis

5a. CONTRACT NUMBER
W81XWH-06-1-0229

5b. GRANT NUMBER
PC051182

5c. PROGRAM ELEMENT NUMBER

6. AUTHOR(S)

Sharron X. Lin, Ph.D.

Email: Sxlin@partners.org

5d. PROJECT NUMBER

5e. TASK NUMBER

5f. WORK UNIT NUMBER

7. PERFORMING ORGANIZATION NAME(S) AND ADDRESS(ES)

The General Hospital Corporation
Massachusetts General Hospital
55 Fruit Street
Boston, MA 02114-2698

8. PERFORMING ORGANIZATION REPORT NUMBER

9. SPONSORING / MONITORING AGENCY NAME(S) AND ADDRESS(ES)
U.S. Army Medical Research
And Material Command
Fort Detrick,
Maryland 21702-5012

10. SPONSOR/MONITOR'S ACRONYM(S)

11. SPONSOR/MONITOR'S REPORT NUMBER(S)

12. DISTRIBUTION / AVAILABILITY STATEMENT

Approve for public release. Distribution unlimited.

13. SUPPLEMENTARY NOTES

14. ABSTRACT

It is fundamentally important to understand the underlying mechanisms regulating prostate caner (PCa) metastasis. Despite the increased PSMA expression found in more advanced stage of PCa, little is known about the functional role of PSMA in PCa progression. With this founding from the Department of Defense Prostate Cancer Research Program, we have achieved each of these tasks during the course of this project. We have been able to (1) monitor PSMA expression in live PCa cells, (2) examine its function in cell adhesion, (3) establish its role in cell migration, (4) identify fibronetin as a specific extracellular matrix for enhanced PSMA-positive cell attachment, (5) determine the association of PSMA with integrin, a key signaling molecule known to controlling cancer progression and metastasis and (6) characterize its enzymatic activity in regulation of cell attachment and migration. Our work has contributed to new insight into the role of PSMA in PCa progression. Knowledge of PSMA in cell adhesion and migration will have a direct impact on the design of targeted treatment for patients suffering metastatic PCa.

15. SUBJECT TERMS
prostate cancer, prostate-specific membrane antigen (PSMA), cell adhesion, cell motility and migration, anti-PSMA antibody, integrin, prostate cancer metastasis

16. SECURITY CLASSIFICATION OF:			17. LIMITATION OF ABSTRACT	18. NUMBER OF PAGES	19a. NAME OF RESPONSIBLE PERSON
a. REPORT	b. ABSTRACT	c. THIS PAGE			19b. TELEPHONE NUMBER *(include area code)*
U	U	U	UU	38	USAMRMC

Table of Contents

Page

Final Report
W81XWH-06-1-0229
P.I., Sharron X. Lin, Ph.D.
Investigating the Functional Role of Prostate-Specific Membrane Antigen and Its Enzymatic Activity in Prostate Cancer Metastasis
Inclusive dates of support 1/31/2006—1/31/2009, unfunded extension to 10/31/2009

INTRODUCTION

PCa metastasis is a multi-step process that involves a variety of molecules affecting the severity of the disease and the response to treatments (1-3). Prostate-specific membrane antigen (PSMA) has been recognized as the single most well-established and highly restricted membrane antigen for PCa and its expression is upregulated approximately 10-fold in advanced stages of metastasis and in hormone-refractory PCa (4-13). These observations indicate the importance of PSMA in PCa and its application in targeted clinical treatments. Little is known about the functional role of PSMA in PCa progression. Previously, we demonstrated that expression of PSMA resulted in morphologically better-spreading cells with redistributed F-actin and beta-1 integrin. Those molecules are known to play key roles in cell adhesion and motility. Furthermore, we observed motility changes in cells with their PSMA enzymatic activity inhibited by specific anti-PSMA antibody. These findings suggest a potential role of PSMA in adhesion and migration, the critical processes during PCa metastasis. Currently, there is no effective treatment for advanced PCa. This proposed study is aimed to establish the role of PSMA and its enzymatic activity in PCa cell adhesion and migration which can be used to develop novel strategies for diagnosis and therapeutic treatment for human metastatic PCa.

BODY

With the funding of the grant, at the original institute (Weill Medical College of Cornell University), we have successfully accomplished the goals proposed in the task 1 and part of the task 2 of the original approved Statement of Work. In the new institute (Harvard Medical School/MGH), we have continued to carry out the proposed work in tasks 2-3 of the approved Statement of Work.

A. Statement of Work (SOW)

The specific tasks of this project are:

Task 1. To characterize the effect of PSMA expression on PCa cell motility and migration

Experiments are designed to test whether increased expression of PSMA in higher-grade cancer is the result of its role in regulating cell motility and migration during PCa metastasis. Changes in cell motility and migration will be measured by *in vitro* 2D and 3D migration assays. Results from these studies will directly indicate the function of PSMA in the particular stages during PCa progression.

Task 2. To determine whether the enzymatic activity of PSMA directly regulates the adhesion and migration of PCa cells

Cell attachment, detachment and migration assays will be performed in the presence or absence of J415, a specific anti-PSMA antibody with measurable inhibitory effect on PSMA enzymatic activity. In addition, a possible link between PSMA enzymatic activity and integrin activity and function will be examined using J415 and P4C10, a functional inhibitory anti-integrin antibody. Demonstrating a connection between PSMA enzymatic activity and integrin activity will advance our understanding of the regulatory machinery controlling PCa metastasis.

With this founding from the Department of Defense Prostate Cancer Research Program, we have achieved each of the proposed tasks during the course of this project. We have been able to (1) monitor PSMA expression in live PCa cells, (2) examine its function in cell adhesion, (3) establish its role in cell migration, (4) identify fibronetin as a specific extracellular matrix for enhanced PSAM-positive cell attachment, (5) determine the association of PSMA with integrin, a key signaling molecule known to controlling cancer progression and metastasis and (6) characterize PSMA enzymatic activity in regulating PCa cell attachment and migration, indicating its role in prostate cancer invasion and metastasis.

B. Background and our previous studies

PCa metastasis is a multi-step process that involves a variety of molecules affecting the severity of the disease and the response to treatments. Increased expression of prostate specific membrane antigen (PSMA) and its enzymatic activity in late-stage and metastatic prostate cancer (PCa) suggest it may play an important role in prostate cancer (PCa) progression. PSMA has been recognized as the single most well-established and highly restricted membrane antigen for PCa and its expression is upregulated approximately 10-fold in advanced stages of metastasis and in hormone-refractory PCa. These observations indicate the importance of PSMA in PCa and its application in targeted clinical treatments. Results from our study have identified and characterized the role of PSMA and its enzymatic activities in cell adhesion and migration, critical in PCa metastasis.

In the recently years, PSMA related study has been one of the focuses for PCa related research. However, its role in PCa progress is yet to be illustrated. We believe that, one of the most critical approaches to identify the role of PSMA is to monitor and examine its role in live prostate caner cells. With this DOD founding, previously, we successfully generated several photo-stable fluorescent probes (Cy3, Cy5, Alexa488, Alexa546 and Alexa633)-conjugated anti-PSMA mAbs (J591 and J415) which directly against the extracellular epitopes of PSMA (14-16). We examined the binding characteristics of these conjugated antibodies and confirmed their unchanged binding properties to live PSMA-positive PCa cells (data shown in Figure 1). With these probes, we were able to monitor PSMA localization and determine its specific role in PCa cells as proposed in this study.

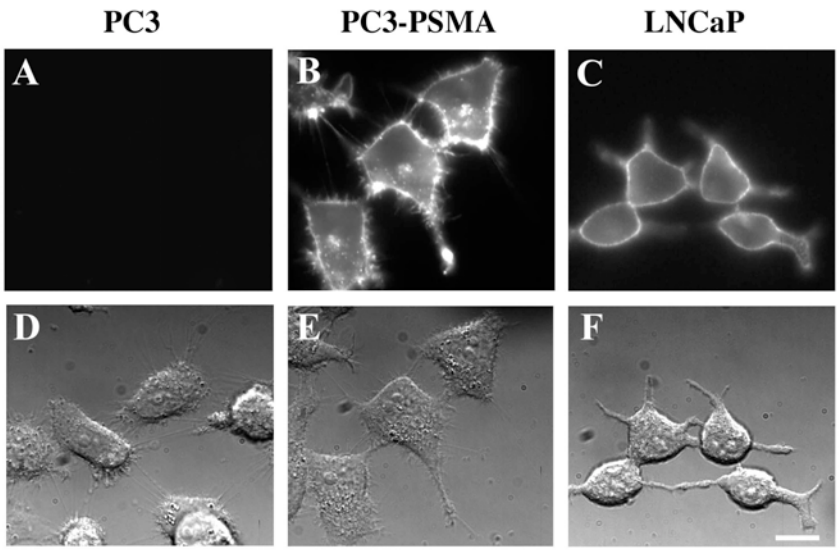

Figure 1. Binding and uptake of Cy3-anti-PSMA Antibody in PC3, PC3-PSMA and LNCaP cells. PC3 cells (A and D), PC3-PSMA cells (B and E) and LNCaP cells (C and F) were incubated with fluorescence-conjugated anti-PSMA antibody Cy3-J591 for 5 min. Cells were rinsed with PBS three times. Live cell images were immediately collected to view the Cy3-J591 labeling (A, B and C). DIC (Differential Interference Contrast) images of the same fields are shown in D, E, and F, respectively. Bar=10μm. **Result**: Specific labeling of anti-PSMA antibody (Cy3-J591) was observed in PSMA-positive PC3-PSMA cells and LNCaP cells but not in PSMA-negative PC3 cells.

To perform live cell experiment, one of the major obstacles was to achieve a reduced PSMA expression for an extended time period. We were able to establish a protocol to reach approximately 90% reduction of PSMA expression by transfecting siRNA against PSMA in LNCaP cells. More importantly, with further modification of this protocol, the reduced PSMA expression in LNCaP cells was maintained for up to 2 weeks. Although various factors were critical for the improvement of siRNA transfection, we found the type of lipid carrier used for the transfection was the most critical. We found Dharmafect3 (Dharmacon) was the most suitable lipid carrier for achieving the highest efficiency in a prolonged period time for PSMA reduction in PSMA-positive LNCaP cells. The results of our work are shown in Figure 2.

Enhanced siRNA transfection efficiency would greatly help to achieve the goals proposed in this study. One of the most important accomplishments during the first period of the funding is that we were able to significantly increase the efficiency of transfection with siRNA of PSMA in LNCaP cells. We established a protocol that not only could achieve an approximately 90% reduction of PSMA expression in LNCaP, but also we were able to further develop a conditional medium to allow LNCaP cell to maintain the reduced PSMA expression for up to 2-weeks. Usually, the effect of transient transfection peaks at 3-5 days after transfection before losing its targeted effect. Achieving a significant reduction of PSMA expression and especially maintaining PSMA expression at a reduced level enabled us to perform the critical functional studies that otherwise won't be possible. This improved protocol achieving high transfection efficiency will have a broader impact on basic prostate cancer research, since LNCaP cell is one of the most commonly cell model systems used for prostate cancer research.

A

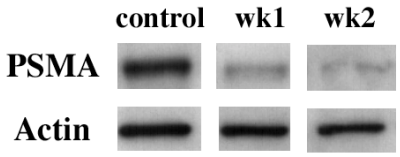

B

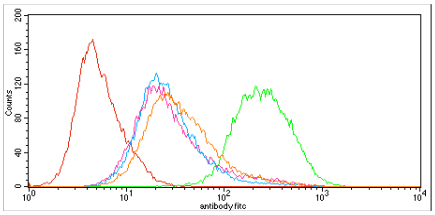

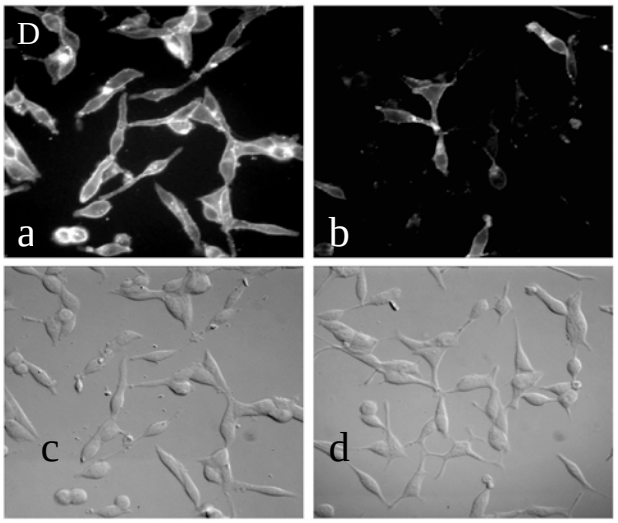

C

Key	Name	Parameter	Gate
	igg ctrl.001	FL1-H	G3
	untreated Incap.001	FL1-H	G3
	2ul dharmafect3.002	FL1-H	G3
	5ul dharmafect3.003	FL1-H	G3
	10ul dharmafect3.004	FL1-H	G3

Figure 2. Reduction of PSMA expression in LNCaP cells by Transfection of siRNA to PSMA. LNCaP cells were transfected with siRNA of PSMA by incubation with a mixture of siRNA and Dharmafect3 for 5 hrs before switching to growth medium (or medium containing 1/3 of the transfection mixture) for indicated period of times. (A), Cell lysate was collected after siRNA transfection for 1 week or 2 weeks and western blot analysis was performed to evaluate PSMA expression. Cell lysate from untransfected LNCaP cells were used as control for normal PSMA levels in LNCaP cells. The level of actin is show for normalization (shown in Figure 2A). FACS analysis was conducted in cells transfected siRNA of PSMA for 3 days with different amount of Dharmafect3 (2-10μl) and the levels of PSMA expression were plotted (shown in Figure 2B-C). In Figure 2D, PSMA-positive LNCaP cells were transfected with siRNA of PSMA for 3 days with Dharmafect3. Cells were then incubated with Cy3-conjugated anti-PSMA antibody J591 before rinses. The staining of J591 in control (a and c) and in siRNA of PSMA transfected cells (b and d) was observed. Panel c-d showed the phase images of the corresponding fluorescence staining in a-b, respectively. **Results**: Significant reduction of PSMA expressions, approximately 90%, was achieved in LNCaP cells transfected with siRNA of PSMA. This reduction of PSMA expression lasted for prolonged period of time.

To understand whether PSMA plays a role in cell attachment and motility, we tested cell adhesion property of PSMA-positive LNCaP cells and PSMA-negative PC3 cells on dishes coated with a range of different substrate materials including: uncoated coverslips without coating or coated with poly-D-lysine, BSA, ECM, fibronectin (FN) and collagen. PCa cell adhesion properties were characterized by examining the morphology of cells and the numbers of cells adhered onto various matrix-coated dishes. By analyzing cell spreading assay an approach previously used to examine the extent of cell adhesion (20), we found that LNCaP attachment was greatly enhanced in dishes coated with FN. Shortly after plating, most of the LNCaP cells were firmly attached onto the FN-coated dishes with well-spread morphology but not onto other extracellular matrices coated dishes. No significant differences in cell adhesion

were observed in PC3 cells plated on dishes coated with any of the above extracellular matrices. These results are shown in Figure 3.

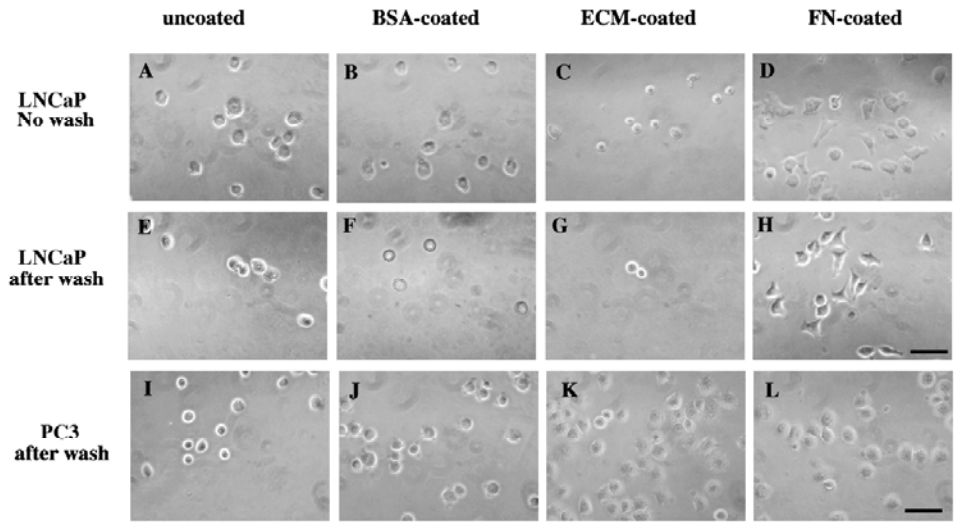

Figure 3. Increased LNCaP adhesion was observed in dishes coated with fibronectin. PSMA-positive LNCaP cells (A-H) and PSMA-negative PC3 cells (I-L) were plated onto triplicates of uncoated dishes (A, E, and I) or dishes coated with 2% BSA (B, F, and J), 10μg/ml extracellular matrix (ECM) (C, G and K) or 10μg/ml fibronectin (FN) (D, H and L). Cells were plated for 60 min without wash (A-D) or washed with serum free RPMI medium 3 times (E-L). After washes, all the inadherent cells were rinsed away, leaving only the adherent cells for imaging collection. Bar=20μm. **Results:** Morphologically better spreading LNCaP cells were observed on FN-coated dishes (D) but not of cells plated on uncoated dishes or dishes coated with either BSA or ECM (A-C, respectively). Enhanced cell attachment and higher number of LNCaP cells were observed on FN-coated dishes after washes (H) when limited numbers of cells were left on uncoated dishes (E) or on dishes coated with either BSA or ECM (F-G, respectively). No significant differences in cell morphology, attachment and cell number were observed of PSMA-negative PC3 cells plated on any of the matrix materials tested (I-L) with or without washes.

These findings suggest a potential interaction between PSMA and specific extracellular matrix molecules. It is known that interactions between integrin and extracellular matrix play a critical role in promoting various cellular functions including cancer progression. In our study, we observed that, among several different extracellular matrices tested, the changes in PSMA-positive PCa cell adhesion were most significant on dishes coated with human fibronectin (FN). Based on the fact that fibronectin is a specific ligand for integrin alpha5-beta1, our results, for the first time, suggested a potential interaction between PSMA and integrin, a key factor shown to regulate many types of cancer progression but yet to be linked in prostate cancer progression. Characterizing the PSMA-positive cell adhesion, especially identifying fibronectin as a specific matrix to enhance the adhesion of LNCaP cells further suggest the role of PSMA in cell attachment and motility. These results will be helpful to select the optimal condition for the adhesion and motility assays proposed in this study.

It is possible that PSMA expression directly regulates cell adhesion therefore to modulate PCa migration, using *in vitro* cell model systems and live-cell imaging methods, we characterized the role of PSMA in cell motility and adhesion. We demonstrated, using wound-healing assay, that PSMA expression reduced cell motility. We monitored and recorded live cells motility of PC3 and PC3-PSMA and observed a significant decrease in the distance of cell migration in PC3 cells expressing PSMA. These data is shown in Figure 4.

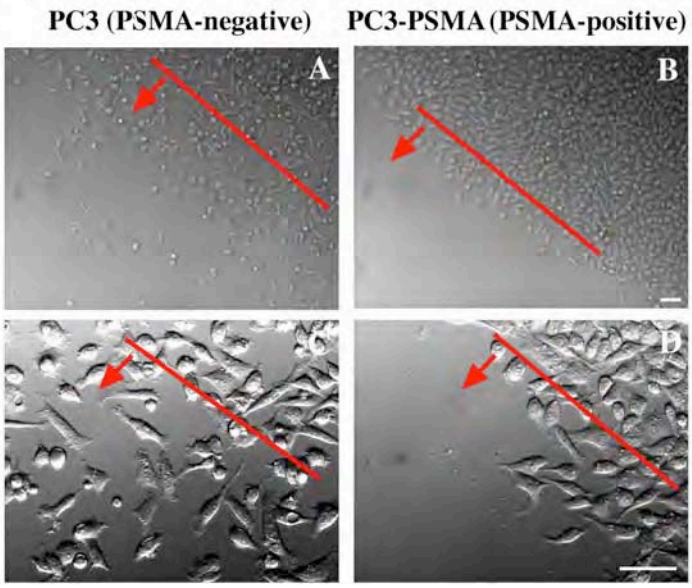

Figure 4. Expression of PSMA in PC3 cells reduces its cell motility. PC3 and PC3 cells stably transfected with PSMA (PC3-PSMA) were grown to confluent monolayer before wounding. Cells were recovered for 1 hour after wounding in regular growth medium and DIC images were collected after 6 hrs in growth medium (A-D). Images in C and D were at a higher (3X) magnification comparing to the images in A and B. The lines indicated the edges of wounded area and the arrows pointed to the direction of cell migration. Bar=20μM. **Result:** Expression of PSMA in PC3 cells slows cell migration.

Actin cytoskeleton network is one of the main components controlling cell motility and it was shown to interact directly with the integrin-mediated cell signaling pathway. To explore the molecular mechanism involved in PSMA regulated cell adhesion and migration, we also investigated if the down stream targets for the integrin-fibronectin signaling were affected. We found PSMA expression had a dramatic effect on the cellular cytoskeleton network with a redistribution of the actin filament. Furthermore, we observed a redistribution of talin, the intermediary that links integrin to the cytoskeleton. These results are shown in Figure 5.

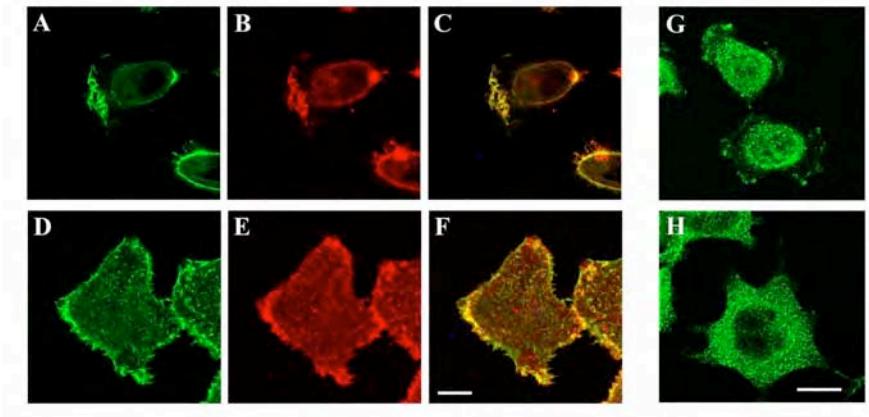

Figure 5. Redistribution of actin filament network in cells expressing PSMA. PC3 cells (A-C and G) and PC3-PSMA cells (D-F and H) were fixed and stained with Alexa488-phalloidin (A and D) for actin network, anti-alpha5-beta1 antibody for integrin alpha5-beta1 (B, E) and anti-talin antibody (G, H) for the distribution of talin. Fields C and F showed the merged images of A-B

and C-D, respectively. **Results**: Expressing PSMA in PC3 cells altered actin-filament network, integrin molecules and talin from polarized distribution to a fragmented and non-polarized distribution.

Together, the above observations (shown in Figure 3-5) provided the direct evidences for the potential role of PSMA in PCa cell adhesion and migration. Identifying fibronectin as a specific matrix to enhance the adhesion of LNCaP cells further imply the role of PSMA in attachment and cell motility. Our data suggested that PSMA regulate cell adhesion by its interaction with the integrin signaling pathways and the actin cytoskeleton. This finding pointed to a new direction for the role of PSMA in prostate cancer progression and may lead to the development of new and targeted treatments for PCa patients.

C. Results

In this proposed study, we further characterize the effect of PSMA expression on PCa cell motility and migration. We illustrated the role of PSMA enzymatic activity on PCa cell adhesion and migration. Results from our study contributed to new insights into the function of PSMA in PCa progression and the knowledge may be used to develop novel strategies for targeted treatment for human metastatic PCa. Details of our findings (shown in figure 6-16) are given in the following sections which are numbered to correspond to the tasks stated in the SOW.

1. Characterization of the effect of PSMA expression on PCa cell motility and migration

It is known that cell adhesion and migration are tightly interconnected. To investigate the relationships between PSMA expression and cell attachment, using *in vitro* cell model systems and live-cell imaging methods, we began to characterize the role of PSMA in cell motility and migration. Using wound-healing assay and live cell imaging and confocal microscope approaches, we recorded cell motility of PC3 and PC3-PSMA (see Figure 6A-B). We found that when live cell migration of these cells was measured (see Figure 6C), a significant decrease in the distance of cell migration was observed in PC3 cells expression PSMA. There were very limited movements in PC3-PSMA cells. These results are consistent with our previous finding of altered F-actin in PC3 cells transfected with PSMA. Expression PSMA in PC3 cells led to redistribution of actin filaments, integrin and talin molecules from polarized to fragmented localization, indicating a transformation of motile cells into less motile but better adhered stationary cells (see Figure 5 of this report). These data suggest that PSMA may be involved in regulating cell adhesion and motility by interacting with the integrin and actin cytoskeleton network

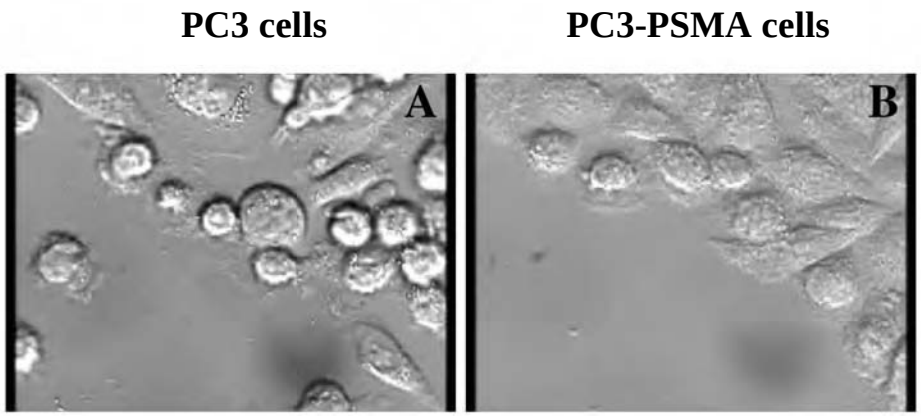

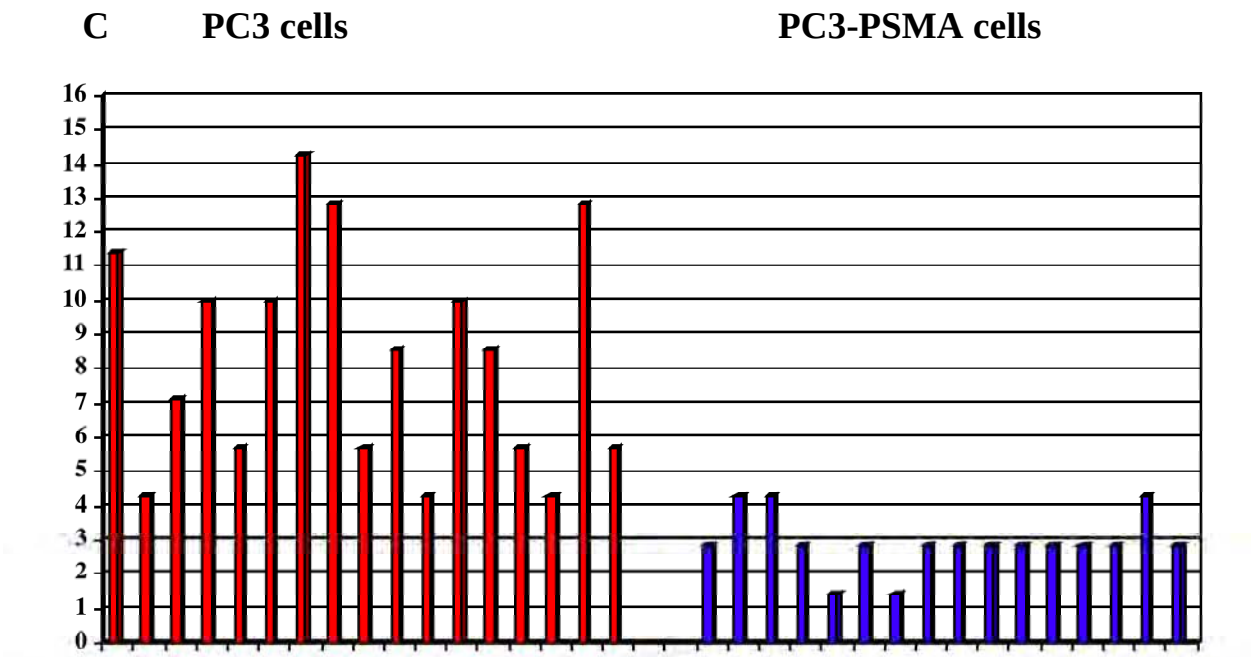

Figure 6. Live cell motility of PC3 and PC3-PSMA cells Live cell motility of PC3 (A) and PC3-PSMA (B) cells was recorded after wounding. Total recording time=30min. In C, the distances of cell migration of PC3 (n=17) and PC3-PSMA (n=16) shown in Figure 6A-B were measured on the migratory tracks produced by individual PC3 and PC3-PSMA cells shown in A-B. The X-axis indicated the individual cells and the Y-axis showed the values of the relative migrating distances of individual cells during the recorded time. **Result:** PSMA expression reduces PC3 cell motility.

In an effort to develop a functional assay to examine the role of PSMA in PCa, we carried out a 2D-wound healing live cell migration assay. We tested if changes in the expression of PSMA were sufficient to alter the PSMA-positive cell motility. As shown in Figure 7, we found that reduction of PSMA expression with siRNA led to significantly higher numbers of cells migrated for longer distance. Further tests conducted with different culture conditions provided additional evidences for this negative-correlation of PSMA expression and cell motility.

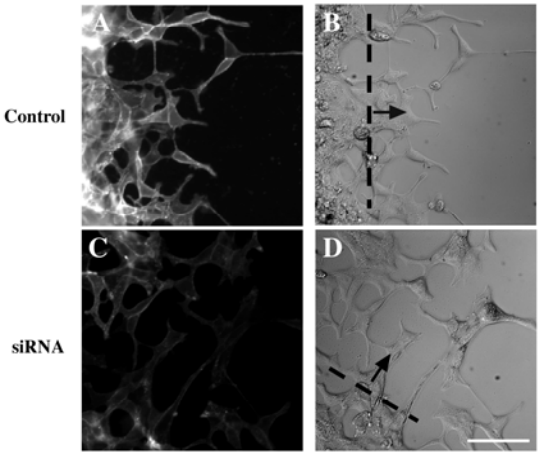

Figure 7. Reduction of PSMA expression increases cell motility. Control LNCaP cells (A-B) and LNCaP cells transfected with siRNA-PSMA (C-D) were grown to confluence before wounding. After wounding, cells were recovered for 1 hr in regular medium then shifted to serum-free medium for 48 hr before DIC images were collected (B, D). The dotted lines indicated the wounded edges and the arrows pointed to the direction of cell migrating. Bar=20μm. **Result:** Reduced expression of PSMA by siRNA increase LNCaP cell motility. Higher numbers of

cells with low PSMA expression migrated faster than those of control-untransfected LNCaP cells.

We further monitor the effect of reduced PSMA expression on cell motility under different cell culture conditions (shown in Figure 8) or under condition that mixed population of LNCaP cells with various levels of PSMA expressions were formed, shown in Figure 9 of this report.

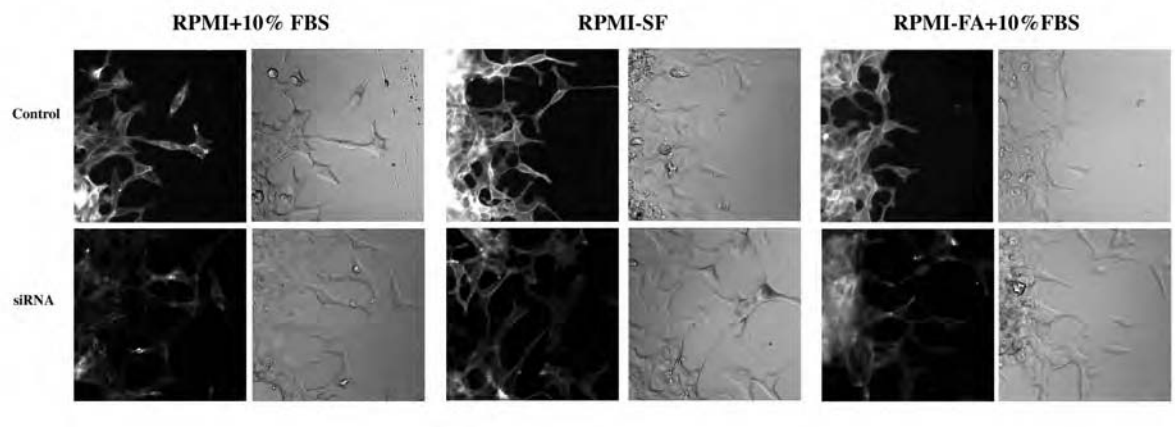

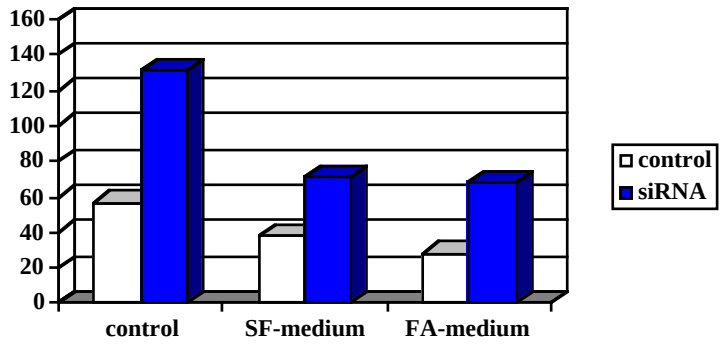

Figure 8. Reduction of PSMA expression increases PSMA-positive LNCaP cell motility Control LNCaP cells or LNCaP cells transfected with siRNA-PSMA were grown until confluence before wounding. After wounding, cells were recovered for 1 hour in regular growth medium then shifted to the various medium (10% FBS, serum-free medium or medium without folate) as indicated above. After 48 hours, the number of cells and the distance of cells migrated (data not shown) were measured and plotted. **Result:** Under all the culture conditions, significant increases of cell migration were observed in cells with reduced PSMA expression by siRNA-PSMA transfection, compared with those of control and non-transfected cells.

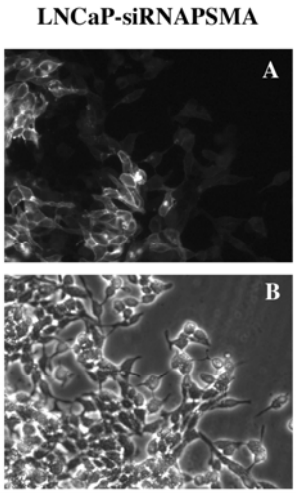

Figure 9. Reduction of PSMA expression increases PSMA-positive LNCaP cell motility. LNCaP cells transfected with siRNA-PSMA were plated onto dishes with high local numbers of cells for colony formation. During the formation and expansion of colonies, a portion of cells started to move outward and appeared at the expanding "edges" of the colonies. PSMA expressions were observed with Alexa546-conjugated J591 (A) and the corresponding DIC images (B) of the same field of cells were collected. **Results:** We observed that, at the expanding edges of the colonies, the majority of the cells that moving outward were the cells with reduced PSMA levels. On

the contrary, cells at the centers (cells with slow motility) showed high levels of PSMA expressions.

Our findings indicated, instead of promoting cell motility, PSMA might function in facilitating cell adhesion. These results shown in Figure 6-9 are consistent with our previous findings that increased cell migration was observed in cells with reduced PSMA expressions.

It is known that cells are connected through a network of molecules and the expression of PSMA on the cell surface not only makes it an attractive target for therapeutic treatment, but also presents its potential to play an important role in PCa progression. In an effort to investigate PSMA-associated molecular mechanisms that regulate PCa cell adhesion, we examined the potential relationships between the expression levels of PSMA and those of integrin alpha5beta1, one of the integrins recognized specifically by fibronectin. We found that PSMA Expressions correlated positively with the levels of integrin alpha5beta1 in PCa cells. Our data provides, for the first time, the evidence for the interaction between PSMA and integrin molecules. These results are shown in Figure 10 of this report.

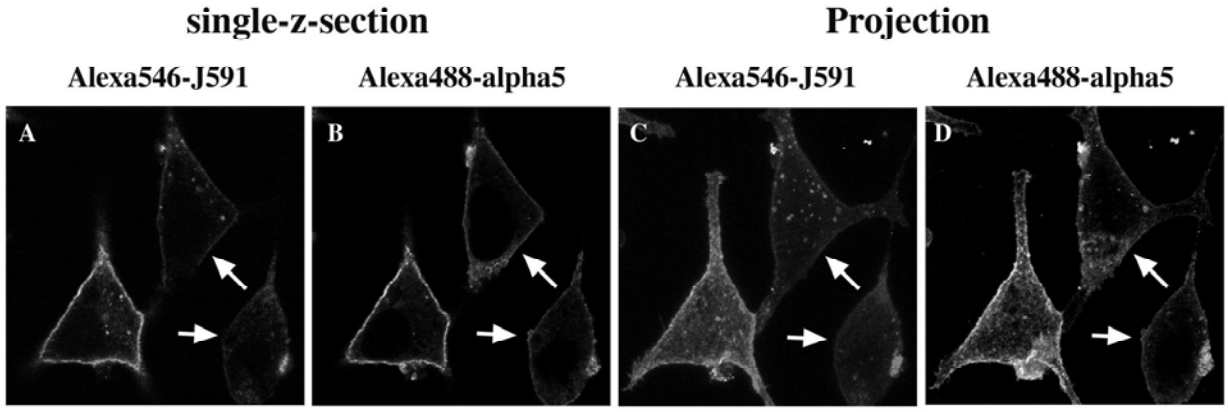

Figure 10. Reduction of PSMA expression correlates with decreased integrin level in LNCaP cells. LNCaP cells (A-D) transfected with siRNA-PSMA were fixed and labeled with monoclonal PSMA antibody Alexa546-J591 (A, C) and polyclonal alpha5 integrin antibody (B, D). Confocal images were collected after labeling. Single sections (A-B) and projected images (C-D) were shown. Arrows pointed to the siRNA-PSMA transfected cells. **Result:** Reduction of PSMA expression by siRNA correlates with decreased integrin alpha5-beta1 levels in LNCaP cell, indicated by arrows.

The activation of integrin molecules requires conformational change. To further characterize the potential interactions between PSMA and integrin alpha5beta1, we used a specific functional blocking anti-integrin alpha5beta1 antibody to examine the effect of integrin alpha5beta1 on PSMA-dependent cell adhesion. As shown in Figure 11, we found decreased numbers of PSMA-positive LNCaP cells with weakened attachment in the present of the anti-integrin alpha5beta1 antibody, while no effect on the adhesion of PSMA-negative PC3 cells was observed under the same experimental conditions. These data provide further evidence for the interactions between PSMA and integrin signaling pathway in PCa progression. These results were presented in the Figure 11 of this report.

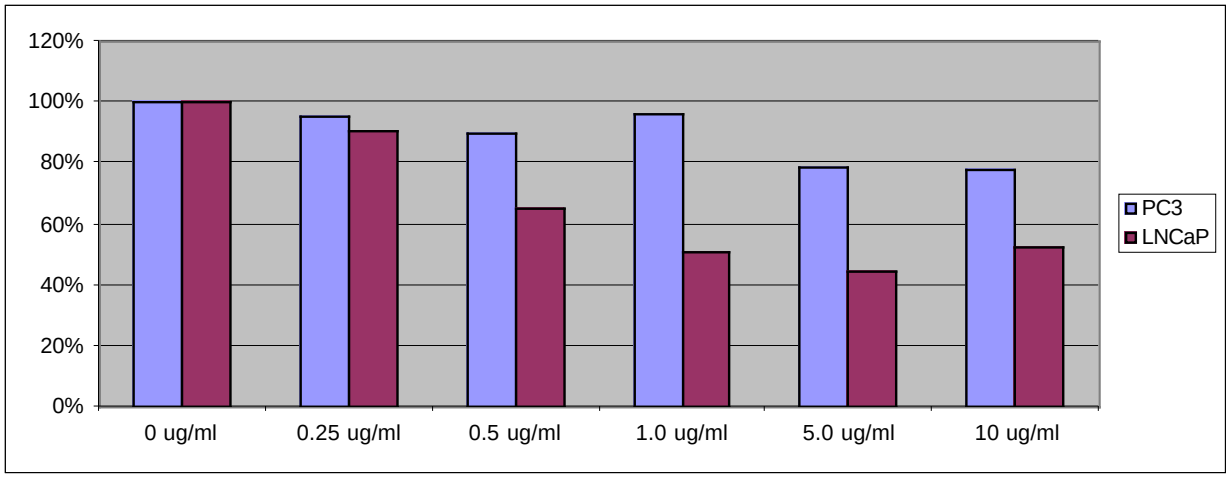

Figure 11. Cell attachment assay with functional blocking anti-integrin antibody
LNCaP cells and PC3 cells were treated with 0-10μg/ml functional blocking anti-integrin antibody before for 15 min before plating onto FN coated coverslips for 60 min. After unattached cells were removed, the numbers and the percentage of cells attached on the dishes were counted, calculated and compared with the control untreated cells (set to be 100%). **Result:** Significant reduction of cell attachment was observed with PSMA-positive LNCaP cells but not with PSMA-negative PC3 cells when treated with functional blocking anti-integrin antibody. Such an effect was shown to be antibody concentration dependent.

These results provided for the first time directly evidence linking PSMA to the integrin-associated signaling pathway which is an important signaling pathway known to play a key role in the progression and metastasis of several types of cancers. Our observation placed this integrin-associated signaling pathway among other pathways identified for regulating PCa progression.

2. PSMA enzymatic activity and PCa cell adhesion and motility

Functionally, PSMA has been classified as a glutamate carboxypeptidase II that possesses two unique enzymatic activities including NAALADase activity (cleaving terminal glutamate from the neurodipeptide, *N*-acetyl-aspartyl-glutamamte NAAG) and folate hydrolase activity that cleaves the terminal glutamate from g-linked polyglutamates. Despite of the variety of strategies used to find out the role of PSMA, the role of PSMA's NAALADase or folate hydrolase activity in normal or tumor prostate is unknown. In this study, with the approaches that alters PSMA expression levels, we demonstrated that PSMA expression negatively regulated cell adhesion and that the integrin signaling pathway may associate with PSMA to regulate cell adhesion, consequently facilitating and promoting PCa progression.

Next, we started to investigate if PSMA enzymatic activity was directly involved in PCa cell adhesion and motility. We used the anti-SPMA specific antibodies (J415 and J591) that bind to the extracellular domain of PSMA specifically and have shown great promise in the ongoing clinical trials. Both antibodies bind with high affinity to PSMA positive LNCaP cells in vitro (30). Humanized J591 has been tested in clinical trials and has demonstrated an ability to image all sites of metastasis, especially in bone with nearly 100% specificity and sensitivity (26-27). Other non-prostate sites of minimal expression are not imaged. Antibody J415 showed 72%

inhibitory effect on PSMA enzymatic activity determined by *in vitro* enzymatic activity assay. When J415 antibodies were used to inhibit PSMA enzymatic activity either *in vitro* or in xenograft models, significant growth inhibitory effect was observed (27-28). To examine the role of PSMA enzymatic activity in PCa cell adhesion and migration, we first measured the level of cellular PSMA enzymatic activity and determined the inhibitory effect of anti-PSMA antibody J415 on PSMA activity. As shown in Figure 12, when uptake of ^{3}H-glutamate by LNCaP in the absence of J415 was defined as 100%, we found that uptake of ^{3}H-glutamate by LNCaP in the presence of J591, J415, and 7E11 was reduced to 68%, 28%, and 86% respectively. No uptake of ^{3}H-glutamate by PSMA negative cells was observed. Anti-PSMA antibody J415 showed the most significant effect on inhibiting PSMA enzymatic activities in PSMA-positive-PCa cells.

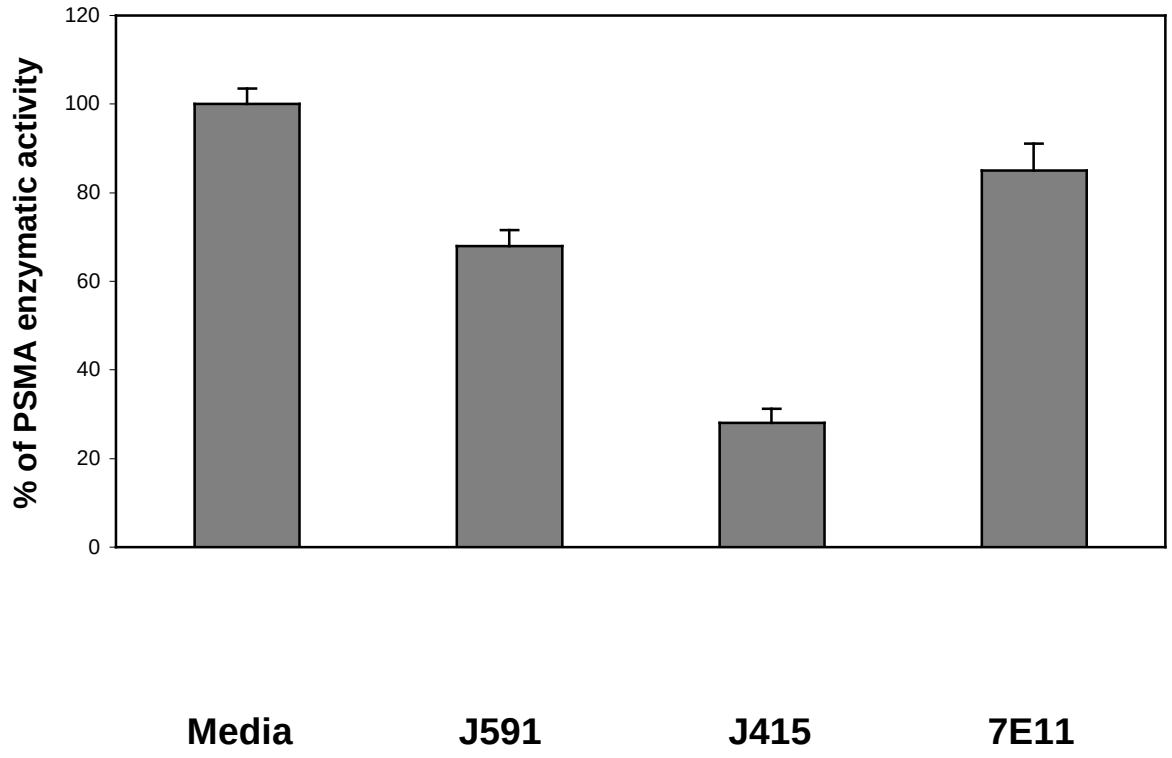

Figure 12. Inhibiting NAALADase activity of PSMA by mAbs LNCaP cells ($10x10^{4}$) were plated on 24-well plates and grown for 2-3 days prior to initiating the experiments. Cells were rinsed in Krebs-Ringer buffer, and incubated with mAbs J591, J415, 7E11 at 10μg/ml in Krebs-Ringer buffer at 37^{0}C for 30 min. ^{3}H-NAAG were co-incubated along with the respective antibody at 0.8 μci/ml for 60 min at 37^{0}C. Cells were washed in Krebs-Ringer buffer, and lysed in 1N of NaOH. Cell lysates were counted in liquid scintillation counter. PSMA negative PC3 cells were as control. **Results**: ^{3}H-NAAG is hydrolysed by PSMA to ^{3}H-glutamate and N-acetylaspartate. ^{3}H-glutamate released from N-acetyl-L-aspartyl-L-glutamate was uptaken by LNCaP cells. Uptake of ^{3}H-glutamate by LNCaP was as 100% in the absence of mAbs. Uptake of ^{3}H-glutamate by LNCaP in the presence of J591, J415, and 7E11 was 68%, 28%, and 86% respectively. No uptake of ^{3}H-glutamate by PC3 cells.

Using the anti-PSMA J415 antibody that showed to inhibit approximately 72% PSMA enzymatic activities, we monitored and characterized the role of PSMA enzymatic activity in PCa cell attachment. We found that reduced PSMA enzymatic activities led to significantly reduced number of PSMA-positive cells attached on to FN-coated dishes. These data suggest that PSMA enzymatic activity are involved in regulating PCa cell adhesion. These results are presented in Figure 13 and Figure 14 of this report.

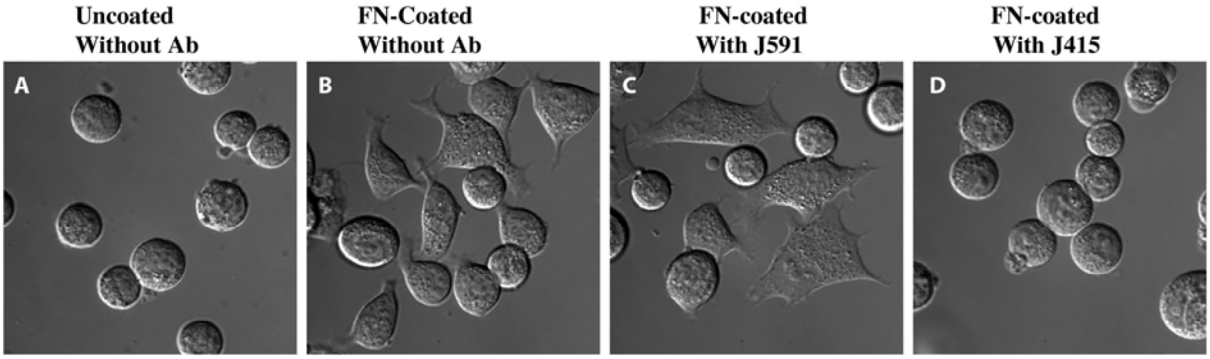

Figure 13. Decreased cell attachment in cell treated with anti-PSMA antibody J451
PSMA-positive LNCaP cell were plated onto dishes with no coating (Figure 13A) or coated with fibronectin (Figure 13 B-D). Cells were then incubated with serum-free medium without any antibody (Figure 13B), or with anti-PSMA antibody J591 (Figure 13C) or J451 (Figure 13D) for 15 min at 37 degree before plated onto the dishes for 45 min. The cells were then rinsed with serum-free medium to remove any unattached cells before DIC images were collected as shown in Figure 13. **Results**: Inhibiting PSMA enzymatic activities reduced cell adhesion.

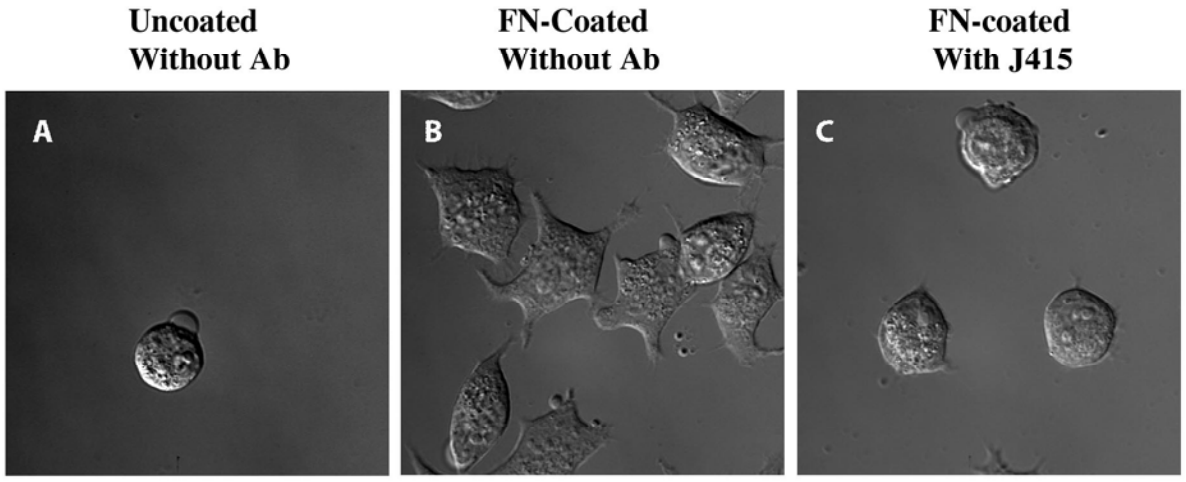

Figure 14. Decreased cell attachment in cell treated with anti-PSMA antibody J451
PSMA-positive LNCaP cell were plated onto dishes with no coating (Figure 14A) or coated with fibronectin (Figure 13 B-C). Cells were then incubated without antibody (Figure 14B), or anti-PSMA antibody J451 (Figure 14C) for 15 min at 37 degree before plated onto the dishes for 60 min. The cells were then rinsed with serum-free medium to remove any unattached cells before DIC images were collected. **Results**: Inhibiting PSMA enzymatic activities decreased cell adhesion.

The effect of reduced PSMA enzymatic activity on cell attachment was further examined with both PSMA-positive LNCaP cells and PSMA-negative PC3 cells for extended time intervals. Similar to the observation we had previously (shown in Figure 13-14), we found that inhibiting PSMA enzymatic activity resulted in reduced cell attachment onto FN-coated dishes. These data are shown in Figure 15 of this report.

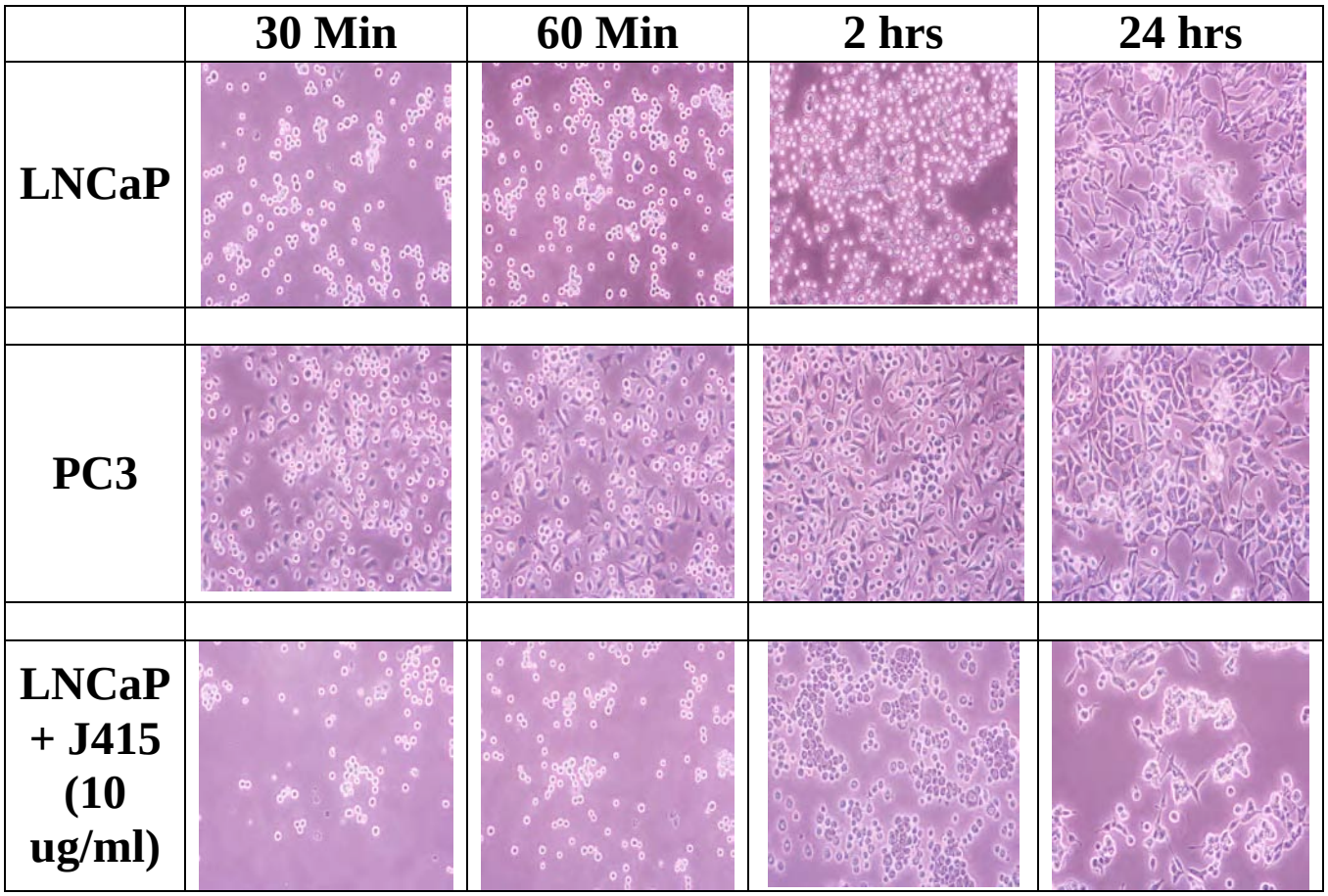

Figure 15. Reduction of PSMA enzymatic activity by anti-PSMA inhibitory antibody J415 decreases PSMA-positive LNCaP cell attachment Equal numbers of LNCaP cells, PC3 cells and LNCaP cells treated with PSMA enzymatic inhibitory antibody J415 at 10mg/ml for 15min before plating were allowed to attach onto dishes for 30min, 60min, 2 hr and 24hrs as indicated. After removal of unattached cells by rinsing the dishes with serum-free medium, the attached cells were counted and images were collected. Representative fields for each condition indicated were shown. **Result:** Significantly reduced numbers of LNCaP cells incubated with J415 were attached onto dishes at all the time points when compared with that of control LNCaP cells. In addition, it appeared that LNCaP cells treated with J415 also displayed a less adherent and more rounded morphology when compared with that of control LNCaP cells.

Together, these data presented in Figure 13-15 strongly suggest the involvement of PSMA enzymatic activity in regulating PSMA-positive PCa cell adhesion.

Once we observed the effect of PSMA enzymatic activities on cell adhesion, we next examined the effect of inhibiting PSMA enzymatic activity on PCa cell motility. These results are shown in Figure 16 of this report.

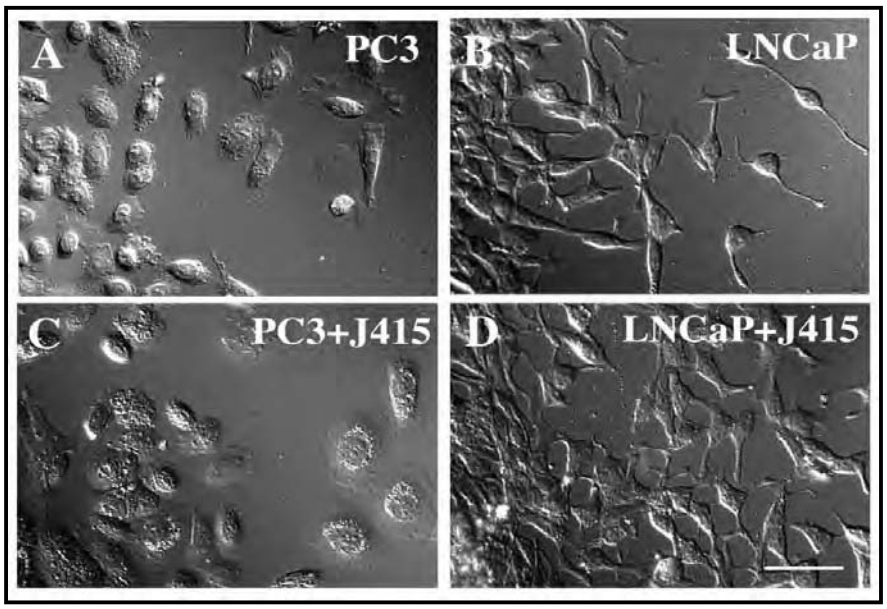

Figure 16. Inhibition of PSMA enzymatic activity increases PSMA-positive LNCaP cell motility. PC3 (A and C) and LNCaP cells (B and D) were grown in regular medium until confluence before wounding. After wounding, cells were grown in medium without folate for 48 hr in the absence (A and B) or the presence (C and D) of anti-PSMA mAb J415 for 48 hours. **Results:** Inhibition of PSMA enzymatic activity increases PSMA-positive cell migration.

E

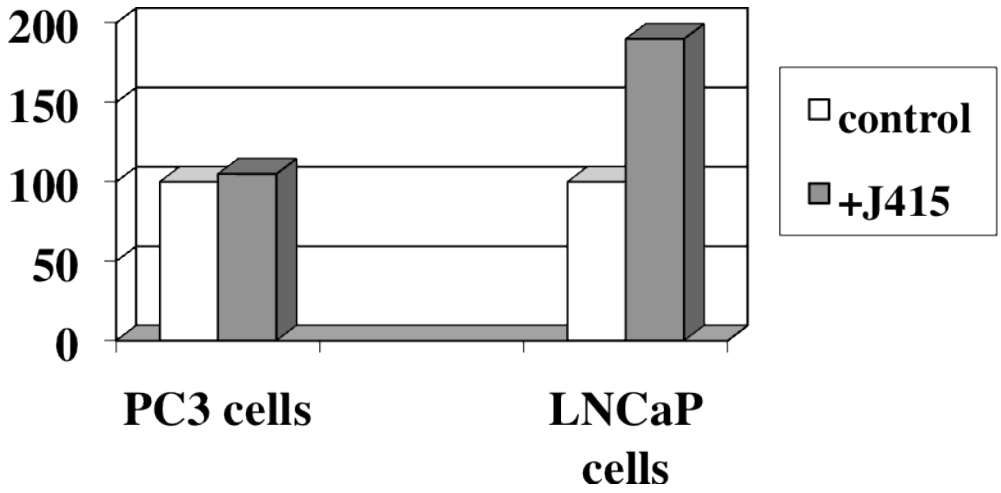

In Figure 16E, the numbers of cells migrated into the wounded area (Figure 16A-B) were considered as 100 % in the absence of J415. The percentages of cells migrated into the wounded area in the presence of J415 were 105% for PC3 cell (Figure 16C) and 190% for LNCaP cells (Figure 16D). **Result**: Inhibiting PSMA enzymatic activity by J415 increases LNCaP cell motility.

KEY RESEARCH ACCOMPLISHMENTS:

1. Demonstrated the difference in cell motility between PSMA-positive and negative cells.
2. Established that reduced PSMA expressions is sufficient to decrease LNCaP cell motility
3. Observed Reduced PSMA expression correlates with decreased integrin alpha5-beta1 levels.
4. Demonstrated the involvement of integrin in PSMA-positive PCa cell adhesion.
5. Observed PSMA enzymatic activity is significantly inhibited by anti-PSMA antibody.
6. Demonstrated the specificity of the effect of PSMA enzymatic activity on the adhesion of PSMA-positive cell.
7. Demonstrated the effect of Inhibition of PSMA enzymatic activity on PCa cell adhesion.
8. Demonstrated the effect of Inhibition of PSMA enzymatic activity on PCa cell motility.

REPORTABLE OUTCOMES:

Published papers and manuscripts:

1. Pan M, Maitin V, Parathath S, Andreo U, Lin SX, St Germain C, Yao Z, Maxfield FR, Williams KJ, Fisher EA. Presecretory oxidation, aggregation, and autophagic destruction of apoprotein-B: a pathway for late-stage quality control. Proc Natl Acad Sci USA. 2008 Apr. 15;105(15):5862-7.2008.

2. Zhang H, Zhang Y, Duan HO, Kirley SD, Lin SX, McDougal WS, Xiao H, Wu CL. TIP30 is associated with progression and metastasis of prostate cancer. Int J Cancer. 15;123(4):810-6. 2008.

Manuscript in preparations for submission and revision:

1. Lin SX, Navarro V, Liu H, and Bander, NH. A functional role of PSMA in prostate cancer cell migration. Manuscript under revisions.

2. Lin SX, Navarro V, Liu H, and Bander, NH. PSMA is involved in cell adhesion by interacting with integrin in prostate cancer cells. Manuscript in preparation.

Presentation and Abstract:

1. Lin, SX, Navarro V, Liu H and Bander NH. A Functional Role of Prostate-Specific Membrane Antigen in Prostate Cancer Metastasis. AACR meeting at Washington DC, 2006.

2. Lin, SX, Navarro V, Sae, K, Liu H and Bander NH. Investigating the Functional Role of Prostate-Specific Membrane Antigen and its Enzymatic Activity in Prostate Cancer Metastasis. IMPACT meeting, Atlanta GA, 2007.

3. Lin, S. X., John, I., Wu, S. L., Schoenfeld, D., Kirley, S., McDougal, W. S. and Wu, C. L. Association of TMPRSS2-ERG Fusion with Surgical Outcome in Clinically Localized Prostate Cancer. 2009. SAC (MGH Scientific Advisory Committee) Scientific Poster presentation, 2009.

CONCLUSION

The goal of the proposal is to investigate the function of PSMA in prostate cancer metastasis. We have made significant progress on several fronts, from establishing the role of PSMA in cells adhesion and motility to discovering and characterizing the relationships between PSMA and the integrin signaling pathway with the extracellular matrix and the actin cytoskeleton, as a result of this founding from the Department of Defense Prostate Cancer Research Program for this project. PSMA will continue to be at the center of research and clinical applications for prostate cancer, due to the fact that it is not only is the single most well-established and highly restricted prostate epithelial cell membrane antigen but its expression progressively increases in higher grade cancers, in hormone-refractory prostate cancers and in metastatic diseases.

Cell adhesion and migration are important components of the metastatic process by facilitating attachment to vascular endothelia, invasion and spreading into secondary tissue sites. Progression of PCa requires repeated adhesion to and detachment from the extracellular matrix microenvironment. And this event is known to be mediated by adhesion molecules. It become evident that well coordinated events that employ various adhesion molecules and receptors, like integrins and its downstream molecules and cytoskeleton components and their regulatory factors are critical in PCa cell motility. Tumor invasion occurs in response to the dysregulation of many of these modulatory points. In this study, for the first time, we provided direct evidences to link PSMA with the integrin signaling pathway. Expression of PSMA in PCa cells altered the localization and expression of integrins, changes the distribution in actin and its related molecules. Such diversity of alterations essential to tumor invasion and metastasis accentuates the importance of understanding the functional role of PSMA in regulating this system.

Since moving to Massachusetts General Hospital/Harvard Medical School, we have worked to complete the aims set in this proposed work. We also started to work with other research groups focusing on prostate cancer, therefore to expand the understanding of PSMA. We have started to collaborate with the Uro-Pathological research group at Massachusetts General Hospital/Harvard Medical School to investigate if PSMA expression contributes to the development of PCa heterogeneity which is the key factor leading to the complexity in PCa diagnosis and treatment.

The outcome from our study will have a direct impact on the improvement of treatments including immunotherapy for human PCa. Knowledge about the action of PSMA in specific event during PCa metastasis will help to design better-targeted approaches for treating patients suffering from metastatic prostate cancer. Currently, monoclonal antibodies against PSMA tested in Phase I-II clinical trials have shown great potential. Identifying the functional role of PSMA in cell adhesion-related events will help to provide guidance for choosing the best suited antibody and the most appropriate toxins for conjugation, therefore to maximize the therapeutic efficacy and reduce side effects for human PCa immunotherapeutic treatment.

REFERENCES:

1. Fidler IJ: Critical determinants of metastasis. Semin. In Cancer Bioloogy 12:89-96, 2002.
2. Paget S: The distribution of secondary growths in cancer of the breast. Lancet 1:571-573, 1889.
3. Fornaro M, Manes T and Languino LR: Integrins and prostate cancer metastases. Cancer Metastasis Rev. 20:321-331, 2001.
4. Israeli RS, Powell CT, Corr JG, Fair WR, Heston WDW. Expression of the prostate-specific membrane antigen. *Cancer Res.* 54: 1807-1811. 1994.
5. Zhang HS, Reuter VE, Slovin SF, Scher HI, Livingston PO. Expression of potential target antigens for immunotherapy on primary and metastatic prostate cancers. *Clin. Cancer Res.* 4: 295-302. 1998.
6. Lopes AD, Davis WL, Rosenstraus MJ, Uveges AJ, Gilman SC. Immunohistochemical and pharmacokinetic characterization of the site-specific immunoconjugate CYT-356 derived from antiprostate monoclonal antibody 7E11-C5. *Cancer Res.* 50: 6423-6429. 1990.
7. Wright GL Jr., Haley C, Beckett ML, Schellhammer PF. Expression of prostate-specific membrane antigen in normal, benign, and malignant prostate tissues. *Urol Oncol.* 1:18-28. 1995.
8. Troyer JK, Beckett ML, Wright GL Jr. Detection and characterization of the prostate-specific membrane antigen (PSMA) in tissue extracts and body fluids. *Int. J. Cancer*. 62:552-558. 1995.
9. Wright GL Jr., Grob M, Haley C, Grossman K, Newhall K, Petrylak D, Troyer J, Konchuba A, Schellhammer PF, Moriarty R. Up-regulation of prostate-specific membrane antigen after androgen-deprivation therapy. *Urology* 48: 326-334. 1996.
10. Silver DA, Pellicer I, Fair WR, Heston WDW, Cordon-Cardo C. Prostate-specific membrane antigen expression in normal and malignant human tissues. *Clin Cancer Res.* 1997, 3: 81-85.
11. Horoszewicz JS, Kawinski E, Murphy GP. Monoclonal antibodies to a new antigenic marker in epithelial cells and serum of prostatic cancer patients. *Anticancer Res.* 7: 927-936. 1987.
12. Israeli, RS, Powell, CT, Fair, WR, and Heston, WD. Molecular cloning of a complementary DNA encoding a prostate-specific membrane antigen. Cancer Res. *53*, 227–230, 1993.
13. Chang, SS, Bander, NH, and Heston, WD. Monoclonal antibodies: will they become an integral part of the evaluation and treatment of prostate cancer–focus on prostate-specific membrane antigen? Curr. Opin. Urol. 9: 391–395, 1999.
14. Ghosh, RH and Maxfield, FR. Evidence for non-vectorial retrograde transferrin trafficking in the early endosomes of Hep2 cells. J. Cell. Bio. 128:549-561, 1995.
15. Ghosh, RH, Mallet, WG, Soe TT, McGraw, TE and Maxfield, FR. An endocytosed TGN38 chimeric protein is delivered to the TGN after trafficking through the endocytic recycling compartment in CHO cells. J. Cell Bio. 142:923-936, 1998.
16. Liu, H, Moy, P, Kim, S, Xia, Y, Rajasekaran, A, Navarro, V, Knudsen, B, and Bander, NH. Monoclonal antibodies to the extracellular domain of prostate-specific membrane antigen also react with tumor vascular endothelium. Cancer Res. 57: 3629–3634, 1997.

17. Gong, MC, Latouche JB, Krause, A, Heston WD, Bander NH and Salelain, M. Cancer patient T cells genetically targeted to prostate-specific membrane antigen specifically lyse prostate cancer cells and release cytokines in response to prostate-specific membrane antigen. Neoplasia. 1(2): 123–127, 1999.

18. Lin, SX, Mallet MG, Huang, AY and Maxfield, FR, Endocytosed cation-independent mannose 6-phosphate receptor traffics via the endocytic recycling compartment en route to the trans-Golgi network and a subpopulation of late endosomes. Mol Biol Cell. 15(2): 721-733. 2004.

19. Lawson MA and Maxfiled FR. Ca and calcineurin-dependent recycling of an integrin to the front of migrating neutrophiles. Nature 377:75-79, 1995.

20. Sood AK, Coffin JE, Schneider GB, Fletcher MS, DeYoung BR, Gruman LM, Gershenson DM, Schaller MD, Hendrix MJ. Biological significance of focal adhesion kinase in ovarian cancer: role in migration and invasion. Am. J. Pathol. 165(4):1087-95. 2004.

21. van der Pluijm G, Sijmons B, Vloedgraven H, van der Bent C, Drijfhout JW, Verheijen J, Quax P, Karperien M, Papapoulos S, Lowik C. Urokinase-receptor/integrin complexes are functionally involved in adhesion and progression of human breast cancer in vivo. Am. J. Pathol. 159:971-82. 2001

22. van der Pluijm G, Vloedgraven HJM, Ivanov B, Robey FA, Grzesik WJ, Gehron Robey P, Papapoulos SE, Löwik CWGM: Bone sialoprotein peptides are potent inhibitors of breast cancer cell adhesion to bone. Cancer Res. 56:1948-1955. 1996.

23. Anikumar G, Rajasekaran SA, Wang S, Hankinson O, Bander NH and Rajasekaran AK. Prostate-specific membrane antigen association with filamin A modulates its internalization and NAALADase activity. Cancer Res. 63:2645-8. 2003.

24. Ghosh A, Wang X, Klein E, and Heston WD. Novel role of prostate-specific membrane antigen in suppressing prostate cancer invasiveness. Cancer Res. 65:727-31. 2005.

25. Chen, HJ, Yuan, J, and Lobel, P. Systematic mutational analysis of the cation-independent mannose 6-phosphate/insulin-like growth factor II receptor cytoplasmic domain. An acidic cluster containing a key aspartate is important for function in lysosomal enzyme sorting. J. Biol. Chem. 272:7003–7012, 1997.

26. Milowsky MI, Nanus DM, Kostakoglu L, Vallabhajosula S, Goldsmith SJ, Bander NH. Phase I trial of yttrium-90-labeled anti-prostate-specific membrane antigen monoclonal antibody J591 for androgen-independent prostate cancer. J. Clin. Oncol. 2004, 22:2522-31.

27. Vallabhajosula S, Smith-Jones PM, Navarro V, Goldsmith SJ, Bander NH. Radioimmuno-therapy of prostate cancer in human xenografts using monoclonal antibodies specific to prostate specific membrane antigen (PSMA): studies in nude mice. Prostate 2004, 58:145-55.

28. Ghosh A, Heston WD. Tumor target prostate specific membrane antigen (PSMA) and its regulation in prostate cancer. J. Cell Biochem. 2004, 91:528-39.

29. Liu H, Rajasekaran AK, Moy P, Xia Y, Kim S, Navarro V, Rahmati R, Bander NH. Constitutive and antibody-induced internalization of prostate-specific membrane antigen. Cancer Res. 1998, 58: 4055–4060.

30. Smith-Jones PM, Vallabahajosula S, Goldsmith SJ, Navarro V, Hunter CJ, Bastidas D, Bander NH. In vitro characterization of radiolabeled monoclonal antibodies specific for the

extracellular domain of prostate specific membrane antigen. Cancer Res. 2000, 60:5237–5243.

APPENDICES:

1. Pan M, Maitin V, Parathath S, Andreo U, Lin SX, St Germain C, Yao Z, Maxfield FR, Williams KJ, Fisher EA. Presecretory oxidation, aggregation, and autophagic destruction of apoprotein-B: a pathway for late-stage quality control. Proc Natl Acad Sci USA. 2008 Apr. 15;105(15):5862-7.2008.

2. Zhang H, Zhang Y, Duan HO, Kirley SD, Lin SX, McDougal WS, Xiao H, Wu CL. TIP30 is associated with progression and metastasis of prostate cancer. Int J Cancer. 15;123(4):810-16. 2008.

Presecretory oxidation, aggregation, and autophagic destruction of apoprotein-B: A pathway for late-stage quality control

Meihui Pan*, Vatsala Maitin*, Sajesh Parathath*, Ursula Andreo*, Sharron X. Lin†, Carly St. Germain‡§, Zemin Yao‡§, Frederick R. Maxfield†, Kevin Jon Williams¶‖, and Edward A. Fisher*‖

*Departments of Medicine, Leon H. Charney Division of Cardiology, and Cell Biology and the Marc and Ruti Bell Vascular Biology and Disease Program, New York University School of Medicine, New York, NY 10016; †Department of Biochemistry, Weill Medical College of Cornell University, New York, NY 10021; ‡Lipoprotein and Atherosclerosis Research Group, University of Ottawa Heart Institute, Ottawa, ON, Canada K1Y 4W7; §Departments of Biochemistry, Microbiology and Immunology, Medicine, and Pathology and Laboratory Medicine, University of Ottawa, Ottawa, ON, Canada K1H 8M5; and ¶Department of Medicine, Division of Endocrinology, Diabetes, and Metabolic Diseases, Thomas Jefferson University, Philadelphia, PA 19107

Communicated by Jan L. Breslow, The Rockefeller University, New York, NY, August 7, 2007 (received for review February 7, 2007).

Hepatic secretion of apolipoprotein-B (apoB), the major protein of atherogenic lipoproteins, is regulated through posttranslational degradation. We reported a degradation pathway, post-ER presecretory proteolysis (PERPP), that is increased by reactive oxygen species (ROS) generated within hepatocytes from dietary polyunsaturated fatty acids (PUFA). We now report the molecular processes by which PUFA-derived ROS regulate PERPP of apoB. ApoB exits the ER; undergoes limited oxidant-dependent aggregation; and then, upon exit from the Golgi, becomes extensively oxidized and converted into large aggregates. The aggregates slowly degrade by an autophagic process. None of the oxidized, aggregated material leaves cells, thereby preventing export of apoB-lipoproteins containing potentially toxic lipid peroxides. In summary, apoB secretory control via PERPP/autophagosomes is likely a key component of normal and pathologic regulation of plasma apoB levels, as well as a means for remarkably late-stage quality control of a secreted protein.

Apolipoprotein-B_{100} (apoB), a 550-kDa glycoprotein, is an essential component of atherogenic plasma lipoproteins (1). Retention, or trapping, of apoB-lipoproteins within the arterial wall is the key initiating event in the pathogenesis of atherosclerosis, the major cause of death world-wide (2–4). Thus, apoB-lipoprotein assembly and secretion, which are often dysregulated (5, 6), attract considerable interest.

ApoB is constitutively synthesized in the liver, and its secretion is controlled mainly through posttranslational destruction. Three processes are known (1, 7, 8): (*i*) endoplasmic reticulum association degradation (ERAD) mediated by the proteasome and stimulated by severe scarcity of lipids for transfer to apoB during its translocation across the ER (1); (*ii*) post-ER presecretory proteolysis (PERPP) (8), a nonproteasomal pathway provoked by diverse metabolic factors *in vitro* and *in vivo*, including intracellular lipid peroxidation (9–14); and (*iii*) receptor-mediated degradation, also known as reuptake, which occurs via interactions of nascent apoB-particles with LDL receptors (8, 10, 15–18) and heparan sulfate proteoglycans (17, 19).

We recently reported that dietary polyunsaturated fatty acids (PUFAs), clinically important lipid-lowering agents, increase presecretory apoB degradation and inhibit apoB secretion from hepatocytes *in vitro* and *in vivo* (9). The effects of PUFAs require their intracellular conversion into lipid peroxides that then trigger the PERPP pathway. Both conventional Ω-6 PUFAs and marine (fish oil) Ω-3 PUFAs, such as docosahexaenoic acid (DHA), have this effect. Antioxidants inhibit apoB degradation in PUFA-treated cells, and thereby enhance the secretion of atherogenic apoB-lipoproteins *in vitro* and *in vivo* (9, 10). In the current study, we sought to identify the novel molecular processes by which PUFA-derived lipid peroxides trigger PERPP of newly synthesized apoB.

Results

PUFA-Treatment of Hepatic Cells Provokes Newly Synthesized apoB to Aggregate Before Its Destruction. Incubation of hepatocytes with DHA or other PUFAs substantially lowers the total (intracellular + secreted) recovery of labeled monomeric apoB (MW ≈550 kDa) owing to stimulation of PERPP (7–9). To characterize the degradative process, we tested approximately two dozen inhibitors against members of the major classes of known intracellular proteases. Surprisingly, none had any significant effect on PUFA-induced loss of newly synthesized labeled monomeric apoB (data not shown).

During these experiments, however, we noticed that PUFAs consistently induced the appearance of material that was precipitated from cellular homogenates by anti-apoB antiserum but exhibited retarded migration on SDS/PAGE relative to monomeric apoB. As shown in Fig. 1, in either rat primary hepatocytes or rat hepatoma McArdle RH-7777 (McA) cells, DHA (complexed to BSA) caused intracellular accumulation of immunoreactive material of high molecular weight in two regions of the lanes: a compact collection within the very top of the stacking gel [large aggregates (LAs)] and a dispersed population between the monomeric apoB band and the interface of the stacking and running gels [intermediate aggregates (IAs)]. ApoB aggregates were not detected in the conditioned media (Fig. 1). Cells treated with either BSA or BSA complexed with oleic acid (OA) contained no or nearly no LAs and much lower amounts of IAs than in DHA-treated cells (Fig. 1).

Homogenates of DHA-treated cells are enriched in lipid peroxides (9) that might artifactually alter apoB after cell lysis. Thus, we prepared homogenates of cells that had been treated with BSA and [^{35}S]methionine (met)/cysteine (cys) in the absence of added fatty acids, i.e., in which little aggregated material should be present. These labeled homogenates were mixed 1:1 either with buffer or with unlabeled homogenates from BSA- or DHA-treated cells, and then subjected to immunoprecipitation and SDS/PAGE. No LAs and no increase in IAs were detected in these mixed homogenates (data not shown). Thus, the aggregates form in intact cells, not after homogenization.

Intracellular abundance of radio-labeled LAs or IAs was directly related to the DHA concentration and a corresponding

Author contributions: M.P., F.R.M., K.J.W., and E.A.F. designed research; M.P., V.M., S.P., U.A., and S.X.L. performed research; C.S.G. and Z.Y. contributed new reagents/analytic tools; M.P., K.J.W., and E.A.F. analyzed data; and M.P., K.J.W., and E.A.F. wrote the paper.

The authors declare no conflict of interest.

‖To whom correspondence may be addressed. E-mail: k_williams@mail.jci.tju.edu or edward.fisher@med.nyu.edu.

This article contains supporting information online at www.pnas.org/cgi/content/full/0707460104/DC1.

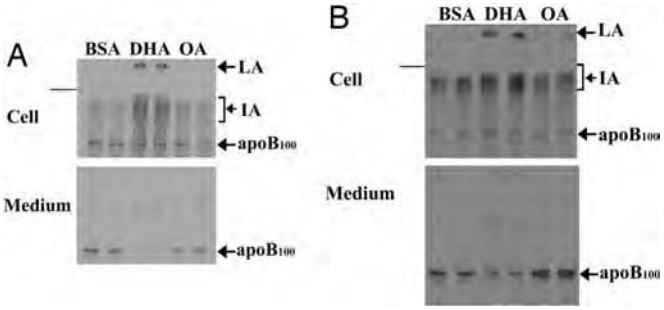

Fig. 1. DHA induces intracellular aggregation of apoB and blocks its secretion, whereas BSA and OA allow release of monomeric apoB into the medium. Primary rat hepatocytes (*A*) or McA cells (*B*) were pretreated for 1 h in medium supplemented with BSA without fatty acids or with DHA or OA (0.6 mM, complexed to BSA) as indicated, and then metabolically labeled to steady-state. Cell lysates (Cell) and medium (Medium) were subjected to anti-apoB immunoprecipitation and SDS/PAGE. Displayed are fluorograms of labeled immunoreactive material. LA, large aggregates; IA, intermediate aggregates; $apoB_{100}$, monomeric apoB. The line to the left of each fluorogram indicates the interface between the stacking and running gels. Each LA band penetrated into the top of the stacking gel.

loss of apoB from the medium (Fig. 2). Quantification of intracellular plus extracellular band intensities demonstrated a remarkably consistent total signal across the DHA concentration range, indicating that the accumulated immunoreactive material inside the cells accounts for the loss of secreted apoB (Fig. 2, line graph).

Two key non-marine PUFAs, arachidonic (ARA) and linolenic (LNA) acids, also inhibit apoB secretion through ROS-dependent PERPP (9). Incubation with either of these fatty acids provoked robust intracellular formation of apoB aggregates [supporting information (SI) Fig. 7]. LNA is unusually potent at inhibiting apoB secretion *in vitro* via PERPP (9), and dietary intake of this fatty acid is linked to low plasma triglyceride levels and decreased cardiovascular risk (20). Of interest, it provoked

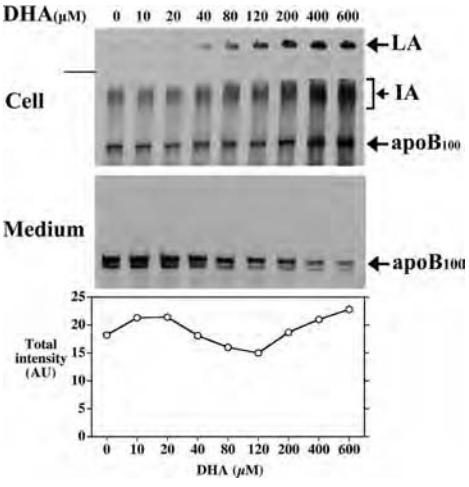

Fig. 2. Dose-response to DHA. (*Top* and *Middle*) McA cells were pretreated for 1 h with the indicated concentrations of DHA and then metabolically labeled to steady-state. Cell lysates and media were subjected to anti-apoB immunoprecipitation and SDS/PAGE. Displayed are resulting fluorograms. Abbreviations and other indicators are as in Fig. 1. (*Bottom*) Intensities of the bands of LAs, IAs, and cellular and secreted monomeric apoB at each DHA concentration from the above fluorograms were determined by densitometry. Sums (cells plus media) were calculated taking into account the difference in exposure time of the two fluorograms (24 h and 12 h, respectively). Data are displayed in arbitrary units (AU).

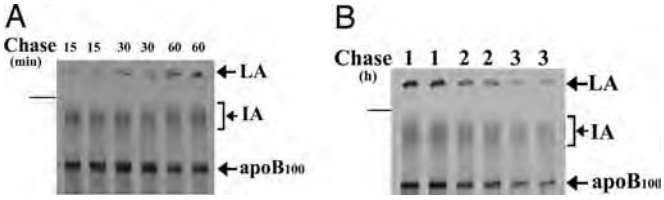

Fig. 3. DHA-induced intracellular aggregates form from monomeric apoB and then gradually disappear over time. McA cells were pretreated for 1 h with DHA/BSA complexes, pulse-labeled for 15 min, and chased for the indicated times. Cell lysates and the corresponding conditioned media were combined 1:1, and apoB contents were analyzed by anti-apoB immunoprecipitation and SDS/PAGE. Fluorograms are shown from short-term (*A*) and long-term (*B*) chases. Abbreviations and other indicators are as in Fig. 1.

the conversion of essentially all monomeric apoB into LAs and IAs by 120 min of chase (SI Fig. 7).

We next performed pulse–chase time courses on DHA-treated McA cells (Fig. 3). During longer chase incubations (Fig. 3*B*), labeled LAs and IAs eventually disappear from the intracellular plus secreted pool. As in Fig. 1, apoB-aggregates do not appear in the medium during 3-h or longer (data not shown) incubations. Taken together, these data indicate that conversion of newly synthesized monomeric apoB into IAs and LAs is required for PUFA-stimulated degradation of the protein.

Large Aggregates Contain apoB That Is Oxidized, and Their Formation Requires Lipid Peroxidation. We focused on the chemical nature of LAs because they are the most extensively aggregated form (Figs. 1–3) and apparently a proximal substrate for degradation (Fig. 3*B*). First, LAs were isolated and analyzed by mass spectroscopy. Peptide sequences from all rat proteins identified as statistically significant are given in SI Table 1. All these sequences corresponded to rat apoB, except for three rat apoA-I peptides. Six distinct apoB peptides appeared beyond residue 2179, which is definitive evidence for rat $apoB_{100}$. Thus, LAs are composed primarily of apoB, with small amounts of apoA-I, a minor component of rat VLDL. No other rat proteins in LAs were detected by this method.

Because ROS play a crucial role in PERPP (9), we assessed oxidative modifications in aggregated apoB. LAs showed strong anti-MDA reactivity, demonstrating oxidized epitopes, whereas IAs and monomeric apoB showed no detectable anti-MDA reactivity (Fig. 4). To establish a causal connection between oxidation and the intracellular formation of apoB aggregates, McA cells were incubated for 2.5 h in [^{35}S]met/cys in the presence of BSA alone, or with DHA, without or with lipid antioxidants or the iron chelator desferrioxamine (DFX). As we report in ref. 9, antioxidants or DFX blocked intracellular TBARS generation and increased the secretion of monomeric apoB (data not shown). Importantly, these treatments also inhibited the formation of both LAs and IAs (Fig. 4*C*). The effect on the amount of LAs was more pronounced, consistent with this species containing the most heavily oxidized apoB (Fig. 4*B*).

Intracellular Trafficking Is Required for apoB Aggregates to Form. Because lipid peroxides trigger intracellular apoB aggregation in intact cells (Fig. 4*C*) but not in cellular homogenates, we hypothesized a role for intracellular trafficking in LA or IA formation. To test this idea, we blocked apoB exit from the ER, using a combination of brefeldin A and nocodazole (BFA/Noc) (21), which we showed to inhibit PERPP (10). Importantly, BFA/Noc only moderately decreased the intracellular content of lipid peroxides in DHA-treated cells (DHA, 81.4 ± 4.3; DHA

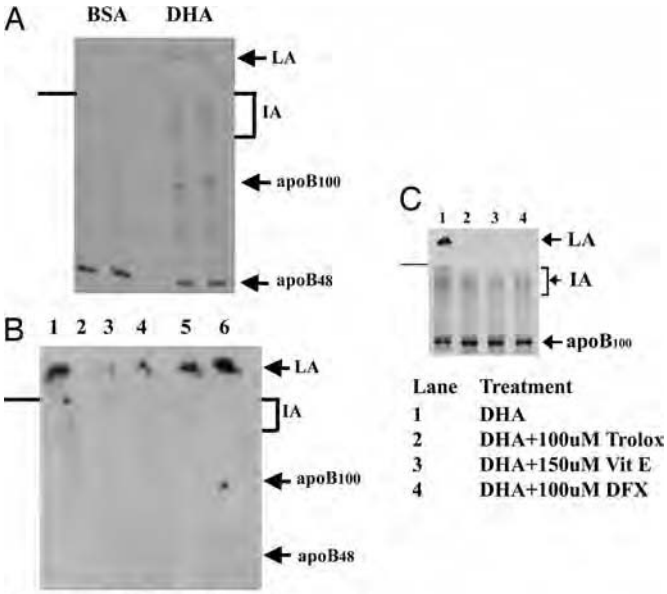

Fig. 4. DHA-induced large aggregates of apoB contain oxidized epitopes and require lipid peroxidation for formation. (*A*) McA cells were incubated for 1 h with BSA or DHA/BSA complexes and then metabolically labeled to steady-state. Cellular lysates and media were subjected to anti-apoB immunoprecipitation and SDS/PAGE and then analyzed by fluorography. (*B*) Lysates from cells treated in parallel, but without the radioactive label, were analyzed by Western blot, using an antibody against MDA. Lane 1, positive control; lane 2, conditioned medium from DHA-treated cells; lanes 3 and 4, lysates of BSA-treated cells; lanes 5 and 6, lysates of DHA-treated cells. Other abbreviations and indicators are as in Fig. 1. (*C*) McA cells were treated with DHA alone or in combination with the indicated lipid anti-oxidants [100 μM Trolox; 150 μM vitamin E (Vit E)] or iron chelator (100 μM DFX). Cells were then metabolically labeled to steady-state. Displayed is a fluorogram after anti-apoB immunoprecipitation/SDS/PAGE analysis of cell lysates.

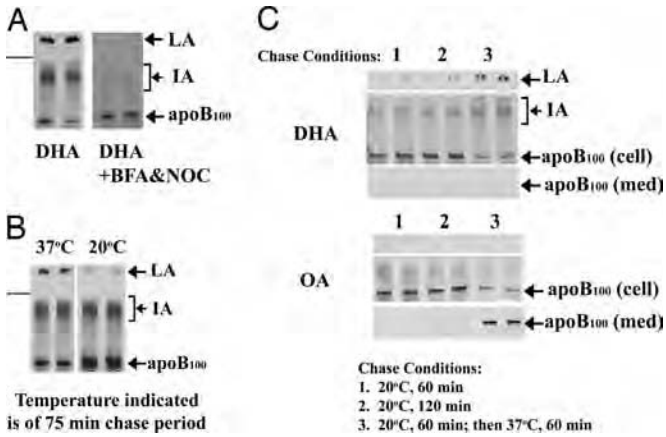

Fig. 5. DHA-induced apoB aggregation requires intracellular trafficking. McA cells were preincubated for 1 h with BSA, DHA, or OA as indicated and then metabolically labeled by a short pulse followed by a chase. Pulse and chase temperatures were 37°C unless otherwise specified. Displayed are fluorograms after anti-apoB immunoprecipitation/SDS/PAGE of cells lysed at the end of the indicated chase periods. (*A*) Effect of blocking apoB exit from the ER. The pulse was 15 min, and the chase was 120 min. To block ER exit, added were nocodazole (Noc) (4 μg/ml, administered 30 min before labeling and then present in the medium thereafter) and brefeldin A (BFA) (2 μg/ml, administered at the start of the chase). (*B*) Effect of cooling to block apoB exit from the Golgi. The pulse was 5 min followed by an 8-min chase to reach the peak of ^{35}S incorporation into apoB. The chase was 75 min at 37°C or 20°C, as indicated. (*C*) Effect of releasing the temperature block. The pulse was 15 min at 20°C. After an initial chase of 60 min at 20°C (Chase 1), the cells in one group of wells were lysed, whereas the rest were extended for another 60 min of chase at either at 20°C or 37°C as indicated (Chase 2).

plus BFA/Noc, 53.3 ± 4.4 pmol of MDA equivalents per milligram of cell protein; $P < 0.01$), but nearly completely blocked the formation of LAs and IAs (Fig. 5*A*). The newly synthesized apoB remained almost entirely monomeric.

Next, we blocked apoB exit from the Golgi in DHA-treated cells. Surprisingly, the standard inhibitor, monensin (5 μM), decreased cellular TBARS by nearly 50%. IAs continued to form in the presence of monensin, but the inhibitor dramatically reduced the level of LAs (SI Fig. 8). To avoid this large effect on ROS, we used a second method: cooling the cells to 20°C, which allows trafficking into, but not out of, the Golgi (22, 23). As a control, cooling OA-treated cells to 20°C blocked all secretion of ^{35}S-labeled apoB (see Fig. 5*C*). Importantly, cooling DHA-treated McA cells to 20°C did not lower the cellular content of lipid peroxides (DHA at 37°C, 60.1 ± 3.7 vs. DHA at 20°C, 80.7 ± 6.1 pmol of MDA equivalents per milligram of cell protein), although, similar to monensin, it allowed continued formation of IAs, but nearly completely inhibited the appearance of LAs (Fig. 5*B*). Bringing the cooled DHA-treated cells from 20°C to 37°C allowed labeled intracellular apoB to be chased into LAs, whereas warming OA-treated cells allowed the intracellular apoB to be chased into the medium in monomeric form (Fig. 5*C*). To verify that impaired formation of LAs at 20°C is not a nonspecific consequence of low temperature, we found that DHA-treated cells cooled to 24°C, which allows proteins to exit from the Golgi (22, 24), formed abundant IAs and LAs (data not shown). Taken together, these results indicate that both IA and LA formation requires lipid peroxidation (Fig. 4*C*) and trafficking out of the ER (Fig. 5*A*) but that LA formation further requires trafficking out of the Golgi (Fig. 5*B*).

Degradation of LAs by the Autophagosomal/Lysosomal System. As shown in Fig. 3*B*, LAs gradually disappeared over several hours. We now revisited the efficacy of several protease inhibitors, none of which was effective at blocking the disappearance of monomeric apoB from DHA-treated cells. Lactacystin, an inhibitor of the proteasome, failed to protect LAs (Fig. 6*A*). In contrast, E64d, an inhibitor of lysosomal/endosomal cathepsins, significantly prolonged the decay of the LA signal (Fig. 6*B*).

The protective effect of E64d implied a lysosomal process, and so we turned our attention to autophagosomes, which transport damaged cytosolic proteins and organelles into lysosomes for degradation (25–27). Autophagosomes were recently shown by Ohsaki *et al.* (28) to be colocalized with a small population of apoB molecules in human Huh-7 hepatoma cells after inhibition of the proteasome (28) and in preliminary reports by Thorne–Tjomsland *et al.* (29) and Tran *et al.* (30) to be induced in hepatic cells treated with Ω-3 fatty acids, perhaps consistent with the known induction of autophagy under prooxidative conditions (25). Addition of 3-methyladenine, which inhibits a PI3-kinase required for autophagosome formation (25, 26), significantly protected LAs in metabolically labeled DHA-treated cells while increasing the IA signal (Fig. 6*B*). This result may explain our prior finding of a role for PI3-kinases in PERPP (8). Likewise, we found that rapamycin, which stimulates autophagosomes by inhibiting the negative regulator mTOR (25, 26), significantly facilitated the degradation of LAs (Fig. 6*C*). None of these inhibitors affected the cellular content of lipid peroxides (data not shown).

To strengthen the relationship between apoB degradation and

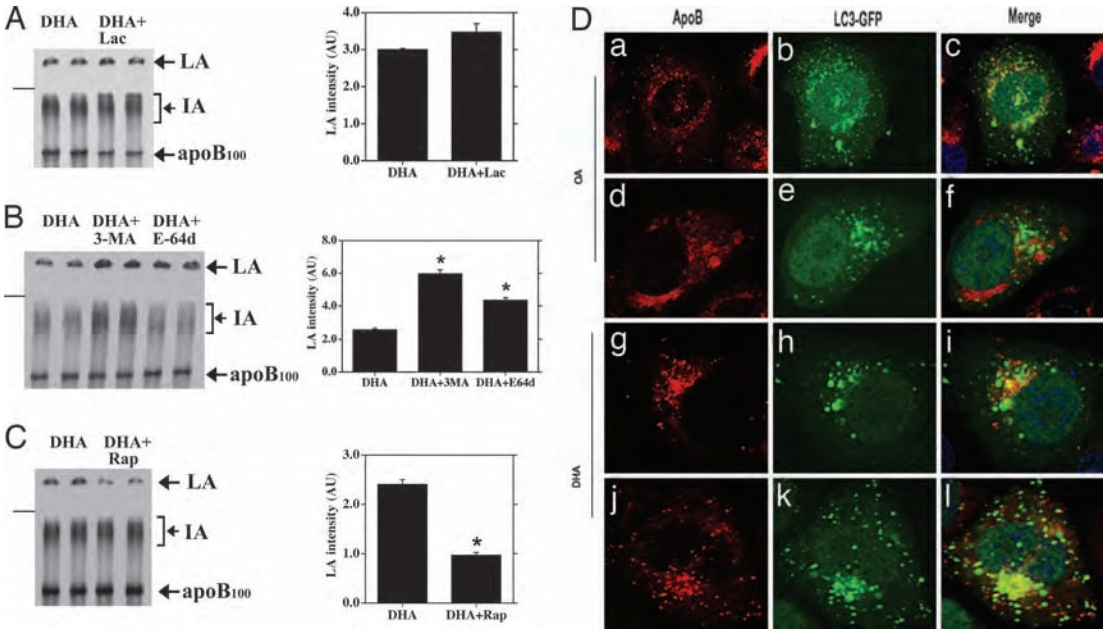

Fig. 6. Involvement of autophagosomes/lysosomes in intracellular degradation of apoB. (*A–C*) McA cells were preincubated with DHA for 60 min and then pulse labeled 37°C for 15 min, followed by a 3-h chase at 37°C to give enough time for labeled LAs to degrade (see Fig. 3). At the end of chase, cells were subjected to anti-apoB immunoprecipitation, SDS/PAGE, and fluorography. Typical fluorograms are displayed at *Left*. (*Right*) Quantifications of intensities of LA bands under different conditions (means ± SEM, $n = 4$). (*A*) Effect of proteasomal inhibition. Lactacystin (Lac) (10 μM) was added 30 min before labeling and kept present in the medium thereafter. The two columns were not significantly different. (*B*) Effect of inhibiting the autophagosome/lysosome system. Ten millimolar 3MA or 10 μM E64d was administered at the start of chase. The columns were significantly different ($P < 0.001$). *, $P < 0.01$ versus the DHA control. (*C*) Effect of stimulation of autophagosomes. Rapamycin (Rap) (250 nM) was added at the start of the chase period. *, $P < 0.0001$. (*D*) McA cells were transfected with an expression plasmid for LC3-GFP. After 24 h, the cells were incubated with either OA (*a–f*) or DHA (*g–l*) for 4 h, after which they were fixed and permeabilzed, and apoB was detected by indirect immunofluorescence (primary antibody, anti-apoB; secondary, goat anti-rabbit conjugated to Texas red). Nuclei were stained blue by DAPI. Laser confocal microscopy of representative cells are shown. Note the colocalization of apoB and LC3 (yellow-orange structures) in the DHA-incubated cells in the juxtanuclear region, which is consistent with the subcellular distribution of autophagosomes and lysosomes.

autophagy, colocalization studies in McA cells were performed taking a standard approach of first expressing, by transient transfection, a GFP-tagged version of the autophagosomal protein LC-3 (31). Then, the transfected McA cells were incubated with BSA complexed to either OA or DHA for 4 h, after which the cells were fixed, permeabilized, and incubated with rabbit anti-apoB antiserum, followed by Texas red-conjugated goat anti-rabbit secondary antiserum. In DHA-incubated cells, laser confocal microscopy revealed areas of colocalization of LC3-GFP and apoB, as illustrated by the yellow-orange structures in representative cells incubated with DHA (Fig. 6*D i* and *l*).

Other evidence (presented in SI Figs. 9–12) in support of a role for autophagy in PUFA-stimulated apoB aggregation and degradation was as follows: (*i*) immunofluorescent microscopy consistent with movement of apoB species into autophagosomes in DHA-treated McA cells: the intracellular apoB signal became concentrated in a juxtanuclear localization (as also seen in Fig. 6*D*), consistent with the subcellular distribution of autophagosomes and lysosomes (SI Fig. 9); (*ii*) the coimmunoprecipitation of LC3 and LAs, and smaller amounts of IAs and monomeric apoB, in DHA-incubated McA cells, with the degree of interaction decreased by DFX cotreatment (SI Fig. 10); (*iii*) increased recovery of the lipidated form of LC3 (LC3-II) in DHA-incubated McA cells (SI Fig. 11); and (*iv*) increased apoB recovery in DHA-treated McA cells that had been transfected with siRNA directed against the essential autophagy protein Atg7 (SI Fig. 12).

Discussion

Based on the present results, we conclude that in hepatic cells lipid peroxides derived from PUFAs provoke limited oxidative modification and aggregation of apoB after its exit from the ER but before it leaves the Golgi. Extensive oxidation and massive aggregation of apoB then occurs but requires trafficking out of the Golgi. Little or none of the oxidized aggregated material leaves the cells. Instead, it is disposed of by autophagosome-lysosomes. The presence of detectable amounts of intracellular apoB-aggregates, even without PUFA supplementation (Figs. 1, 2, and 5), extends our earlier demonstrations of ROS-dependent control of apoB secretion in the basal state, indicating broad physiologic importance (9, 10). Thus, the PERPP pathway appears to be not only a major regulator of hepatic apoB secretion but also a means for remarkably late-stage quality control of an endogenous protein after it has left the ER.

Prior studies on quality control in the secretory pathway have focused on preventing the exit of malfolded proteins from the ER (reviewed in ref. 32). In contrast, studies on autophagosomes have emphasized their importance in degradation of the cytosol, including long-lived proteins, superfluous or damaged organelles, and overflow from ERAD (25–27). We doubt that autophagic degradation of apoB is a consequence of ERAD being overwhelmed, because analysis of LAs by mass spectroscopy did not detect ubiquitin. Rather, the autophagic process appears to represent a role in secretory regulation of apoB independent from ERAD, as suggested in refs. 30 and 33. The reason may be that PUFAs, an essential part of the diets of herbivores and omnivores, are readily converted into lipid peroxides inside cells. Although one physiologic response to PUFA-rich diets is the induction of anti-oxidant enzymes in the liver (34), our results suggest that another physiologic response is the aggregation and then destruction of a portion of newly synthesized apoB.

This selective destruction of some of the apoB late in the secretory pathway (Fig. 5) is consistent with demonstrations that

full lipidation of apoB-lipoproteins to VLDL buoyancy occurs post-ER (35–37). Also, given the conspicuous physical barriers against translocating large, extensively lipidated apoB-lipoproteins out of the secretory pathway, which would be required for the proteasome to have access to them, the autophagosomal/lysosomal system may be the only plausible mechanism for late-stage quality control of these particles. Although we have implicated autophagy in apoB-PERPP and have localized the later steps of the pathway to the Golgi and beyond, still to be determined are the source (e.g., mitochondria, microsomal cytochrome P450 enzymes, and peroxisomes) of the modifying free radicals and where and how they first encounter apoB.

Besides protecting the liver from potentially toxic aggregates (38), destruction of these particles may also prevent the export of lipid peroxides on VLDL to triglyceride-consuming, but oxidant-sensitive, tissues in the periphery, such as cardiac muscle (39). Thus, lipid peroxidation is kept within the liver, where it is safe, even beneficial (40), and away from potentially vulnerable peripheral organs. Reverse transport of oxidized or oxidizable lipids from periphery to liver could serve a similar function (9, 41).

Regardless of teleologic explanations, hepatocytes have adapted an ancient eukaryotic process, autophagy, to the quality control of a comparatively recent structure, the large, lipidated, post-ER apoB-lipoprotein, especially in response to metabolic perturbation. ApoB may be particularly susceptible to modification by lipid peroxides inside hepatocytes, both because it would be assembled into close contact with them and because the unique structure of apoB facilitates its aggregation under a wide range of physiologic (e.g., Figs. 1 and 2), pathogenic, and even artificial stimuli that do not affect other proteins to the same extent (4, 42–47). Its remarkable susceptibility to aggregation allows a normal hypolipidemic response to dietary PUFAs and other stimuli (Fig. 1 and refs. 8–11 and 14) but unfortunately may also contribute to the aggregation, retention, and atherogenicity of apoB-lipoproteins once they reach the vessel wall (2, 4). Defects in PERPP, then, might produce significant health risks through hepatic oversecretion of highly atherogenic apoB-lipoproteins, a key feature of the metabolic syndrome.

Taken together, the data here and in previous reports suggest that under typical conditions, apoB escapes ERAD (8), but then autophagy serves as a quality control process for handling adverse modifications of apoB and VLDL that occur late in the secretory pathway as consequences of the normal processing of PUFAs and their intracellular peroxidized byproducts. Secretory control via PERPP/autophagosomes likely represents a key component of normal and pathologic regulation of plasma apoB levels, given that PUFAs are a major component of the heart-healthy lifestyle owing to their lipid-lowering properties (40) and that many diseases of apoB oversecretion have become a major health problem (6).

Experimental Procedures

General Materials. Male Sprague–Dawley rats were purchased from The Jackson Laboratory. Unless otherwise specified, reagents were from Sigma. [^{35}S]methionine/cysteine ([^{35}S]met/cys) was from Perkin–Elmer. Collagenase was from Worthington Biochemical. Rabbit polyclonal antiserum against rat apoB was developed in the authors' laboratory. Complete protease inhibitor mixture with EDTA was from Roche. Autofluor was from National Diagnostics. McA cells were obtained from the American Type Culture Collection.

Cell Culture. Rat primary hepatocytes were prepared as in ref. 8, using a protocol approved by the Institutional Animal Care Committee. Hepatocytes were plated in six-well plates precoated with type I collagen and maintained in Waymouth's medium (Waymouth's MB 752/1 containing 1% streptomycin/penicillin, 1% L-glutamine, 0.2% BSA, and 0.1 nM insulin). After 12–14 h incubation, the primary hepatocytes were subjected to study protocols.

McA cells were plated in six-well plates or 100-mm Petrie dishes and maintained in complete DMEM, which was changed every 3 days. When cells reached ≈90% confluence, they were used for the experiments.

Culture media were supplemented with fatty acids, typically at a final concentration of 0.6 mM given as a complex with BSA (fatty acid:BSA molar ratio = 5:1), as described (e.g., ref. 48). PUFAs to stimulate PERPP were DHA, ARA, and LNA (8, 9). OA complexed to BSA, or BSA (0.12 mM) without fatty acids, served as controls. Unless otherwise noted, cells were incubated at 37°C in 5% CO_2. For inhibition of protein trafficking, the temperature in some experiments was lowered to either 20°C (22, 23) or 24°C.

Metabolic Labeling. ***Steady-state labeling of hepatic proteins.*** After the pretreatments described in the figure legends, endogenous proteins were metabolically labeled to steady-state (49) by incubating hepatocytes at 37°C for 3 h in met/cys-free DMEM-complete (met/cys-free high-glucose DMEM with 0.5% FBS, 0.5% horse serum, 1% streptomycin/penicillin, and 1% L-glutamine) supplemented with 100 μCi [^{35}S]met/cys per ml of medium and various compounds indicated in *Results*.

Pulse–chase studies. After the pretreatments described in the figure legends, cellular proteins were metabolically labeled with met/cys-free DMEM-complete (see above) supplemented with 200–400 μCi [^{35}S]met/cys per milliliter of medium and various compounds indicated in *Results*. The temperature and duration of labeling and the chase periods varied according the experimental goals and are shown in the appropriate figure legends.

After the labeling period, the media were removed, and the cells were washed twice with PBS at the same temperature as the chase incubation and then incubated with excess unlabeled met (10 mM)/cys (3 mM) in chase medium (for primary hepatocytes, Waymouth's MB 752/1 containing 1% streptomycin/penicillin, 1% L-glutamine, 0.2% BSA, and 0.1 nM insulin; for McA cells, high-glucose DMEM containing 0.5% FBS, 0.5% horse serum, 1% penicillin/streptomycin, and 1% L-glutamine).

Immunoprecipitation, Electrophoresis, and Fluorography. Plates or dishes of cells were placed on ice. Media were collected and supplemented with PMSF (1 mM). Cells were washed three times with cold PBS. Cell lysis buffer [10 mM PBS (pH 7.4), 125 mM NaCl, 36 mM lithium dodecyl sulfate, 24 mM deoxycholate, and 1% Triton X-100] freshly supplemented with protease inhibitor mixture and 1 mM PMSF was used to lyse cells. Both cellular lysates and media were spun at 10,000 $\times$ *g* for 5 min to remove debris. One percent of each lysate and medium sample was treated with trichloroacetic acid (TCA) at 4°C, and the precipitates were resuspended and counted to quantify total ^{35}S-labeled proteins (8). The remaining lysate and medium samples were subjected to apoB immunoprecipitation.

As previously, we focused on $apoB_{100}$, because it is the form of apoB that is secreted from human liver and is the predominant form of rat hepatic apoB on large, lipid-rich lipoproteins (50), the targets of PERPP (8). In addition, the effect of PUFAs on total $apoB_{48}$ recovery has been small in prior and the present studies (data not shown), owing to its under-representation in large lipid-rich particles (8, 48). As indicated in *Results*, depending on the experiment, either the total amount of labeled $apoB_{100}$ (intracellular plus secreted) or the separate recoveries from cells or conditional media were determined by immunoprecipitation followed by SDS/PAGE/fluorography/densitometry, as described in ref. 9.

Detection of MDA-Modified apoB. Cellular content of lipid peroxides was determined by measuring thiobarbituric acid-reactive substances (TBARS) as described in ref. 9. Results are expressed as malondialdehyde (MDA) equivalents normalized to cellular protein mass (DC protein assay kit; Bio Rad).

For immunodetection of oxidatively modified intracellular apoB, cells were incubated for 4 h in DMEM supplemented with 0.5% FBS, 0.5% horse serum, 1% L-glutamine, and 1% penicillin/streptomycin with 0.12 mM BSA or 0.6 mM DHA. After the preincubation, steady-state labeling with [^{35}S]met/cys was done as above but in the presence of the corresponding BSA and DHA treatments.

At the end of the labeling period, treatment media were collected, cells were washed twice with PBS, and lysed. ^{35}S-labeled apoB was then immunoprecipitated from cell lysates.

Aliquots of immunoprecipitates (normalized according to total TCA-precipitable counts) were resolved on two separate gels. One gel was subjected to fluorography, and the other was used to transfer proteins to Polyscreen PVDF membrane (Perkin–Elmer). Rabbit anti-MDA (Alpha Diagnostic) primary antibody (1:1,000) was followed by anti-rabbit IgG-peroxidase (1:10,000; Sigma). Detection was by Western Lightning Chemiluminescence reagent plus kit (Perkin–Elmer). MDA-Ovalbumin (Alpha Diagnostic) was the positive control.

Colocalization Studies. McA cells were transfected with an expression plasmid for LC3-GFP [a generous gift from T. Yoshimori (National Institute of Genetics, Mishima, Japan)] using the TransIT reagent (Mirus Bio), following the manufacturer's protocol. After 24 h, cells were then replated on collagen-coated chambered slides. After 2 h to allow attachment, cells were then incubated for 4 h at 37°C with BSA complexed to either OA (0.6 mM) or DHA (0.6 mM). Cells were fixed with 3.3% paraformaldehyde and then permeabilized with 0.1% Triton X-100. Cells were incubated with rabbit anti-rat apoB serum (1:250). After washing, cells were next incubated with Texas red-conjugated goat anti-rabbit secondary antibody (1:250; Jackson ImmunoResearch). Nuclei were stained with DAPI (Vector Laboratories). Cells were imaged with a Zeiss 510 Meta laser scanning confocal microscope with a 63× Plan-Apochromat NA 1.4 objective and the digitized files processed by Adobe Photoshop 5.5.

Statistical Analyses. Unless otherwise noted, quantitative results are displayed as mean ± SEM, $n = 4$. For most comparisons, two-tailed t tests were used. For comparisons involving several groups, ANOVA was initially used, and, when indicated, pairwise comparisons of each experimental group versus the control group were performed using the Dunnett q' statistic (51).

ACKNOWLEDGMENTS. We thank Ms. Cristina Villagra for technical assistance, Dr. Chris Cardozo (Mount Sinai School of Medicine, New York, NY) for advice on protease inhibitors, and Dr. Ana Maria Cuervo (Albert Einstein College of Medicine, Bronx, NY) for advice and protocols in the area of autophagy. This work was supported by National Institutes of Health Grants HL58541 (to E.A.F.), HL73898 and HL56984 (K.J.W.), and DK27083 (F.R.M.).

1. Fisher EA, Ginsberg HN (2002) Complexity in the secretory pathway: the assembly and secretion of apolipoprotein B-containing lipoproteins. *J Biol Chem* 277:17377–17380.
2. Williams KJ, Tabas I (1995) The response-to-retention hypothesis of early atherogenesis. *Arterioscler Thromb Vasc Biol* 15:551–561.
3. Skålén K, *et al.* (2002) Subendothelial retention of atherogenic lipoproteins in early atherosclerosis. *Nature* 417:750–754.
4. Williams KJ, Tabas I (2005) Lipoprotein retention—and clues for atheroma regression. *Arterioscler Thromb Vasc Biol* 25:1536–1540.
5. Grundy SM, Chait A, Brunzell JD (1987) Familial combined hyperlipidemia workshop. *Arterioscler Thromb Vasc Biol* 7:203–207.
6. Parhofer KG, Barrett PH (2006) Thematic review series: patient-oriented research. What we have learned about VLDL and LDL metabolism from human kinetics studies. *J Lipid Res* 47:1620–1630.
7. Williams KJ, Fisher EA (2001) Atherosclerosis: cell biology and lipoproteins–three distinct processes that control apolipoprotein-B secretion. *Curr Opin Lipidol* 12:235–237.
8. Fisher EA, *et al.* (2001) The triple threat to nascent apolipoprotein B. Evidence for multiple, distinct degradative pathways. *J Biol Chem* 276:27855–27863.
9. Pan M, *et al.* (2004) Lipid peroxidation and oxidant stress regulate hepatic apolipoprotein B degradation and VLDL production. *J Clin Invest* 113:1277–1287.
10. Jiang XC, *et al.* (2005) Phospholipid transfer protein deficiency impairs apolipoprotein-B secretion from hepatocytes by stimulating a proteolytic pathway through a relative deficiency of vitamin E and an increase in intracellular oxidants. *J Biol Chem* 280:18336–18340.
11. Qiu W, Avramoglu RK, Rutledge AC, Tsai J, Adeli K (2006) Mechanisms of glucosamine-induced suppression of the hepatic assembly and secretion of apolipoprotein B-100-containing lipoproteins. *J Lipid Res* 47:1749–1761.
12. Uchiyama S, Shimizu T, Shirasawa, T (2006) CuZn-SOD deficiency causes ApoB degradation and induces hepatic lipid accumulation by impaired lipoprotein secretion in mice. *J Biol Chem* 281:31713–31719.
13. Chirieac DV, Davidson NO, Sparks CE, Sparks JD (2006) PI3-kinase activity modulates apo B available for hepatic VLDL production in apobec-$1^{-/-}$ mice. *Am J Physiol Gastrointest Liver Physiol* 291:G382–G388.
14. Ng CJ, *et al.* (2006) Paraoxonase-2 deficiency aggravates atherosclerosis in mice despite lower apolipoprotein-B-containing lipoproteins: Anti-atherogenic role for paraoxonase-2. *J Biol Chem* 281:29491–29500.
15. Williams KJ, Brocia RW, Fisher EA (1990) The unstirred water layer as a site of control of apolipoprotein B secretion. *J Biol Chem* 265:16741–16744.
16. Williams KJ, Petrie KA, Brocia RW, Swenson TL (1991) Lipoprotein lipase modulates net secretory output of apolipoprotein B in vitro. A possible pathophysiologic explanation for familial combined hyperlipidemia. *J Clin Invest* 88:1300–1306.
17. Williams KJ, *et al.* (1992) Mechanisms by which lipoprotein lipase alters cellular metabolism of lipoprotein(a), low density lipoprotein, and nascent lipoproteins. Roles for low density lipoprotein receptors and heparan sulfate proteoglycans. *J Biol Chem* 267:13284–13292.
18. Millar JS, *et al.* (2005) Complete deficiency of the low-density lipoprotein receptor is associated with increased apolipoprotein B-100 production. *Arterioscler Thromb Vasc Biol* 25:560–565.
19. Fuki IV, *et al.* (1997) The syndecan family of proteoglycans. Novel receptors mediating internalization of atherogenic lipoproteins *in vitro*. *J Clin Invest* 100:1611–1622.
20. Djousse L, *et al.* (2003) Dietary linolenic acid is inversely associated with plasma triacylglycerol: The National Heart, Lung, and Blood Institute Family Heart Study. *Am J Clin Nutr* 78:1098–1102.
21. Lippincott-Schwartz J, Yuan LC, Bonifacino JS, Klausner RD (1989) Rapid redistribution of Golgi proteins into the ER in cells treated with brefeldin A: Evidence for membrane cycling from Golgi to ER. *Cell* 56:801–813.
22. Saraste J, Kuismanen, E (1984) Effect of monensin on the assembly of Uukuniemi virus in the Golgi complex. *Cell* 38:535–549.
23. Griffiths G, *et al.* (1989) The dynamic nature of the Golgi complex. *J Cell Biol* 108:277–297.
24. Tartakoff AM (1986) Temperature and energy dependence of secretory protein transport in the exocrine pancreas. *EMBO J* 5:1477–1482.
25. Meijer AJ, Codogno, P (2004) Regulation and role of autophagy in mammalian cells. *Int J Biochem Cell Biol* 36:2445–2462.
26. Kirkegaard K, Taylor MP, Jackson WT (2004) Cellular autophagy: surrender, avoidance and subversion by microorganisms. *Nat Rev Microbiol* 2:301–314.
27. Yorimitsu T, Klionsky DJ (2005) Autophagy: Molecular machinery for self-eating. *Cell Death Differ* 12 (Suppl 2):1542–1552.
28. Ohsaki Y, Cheng J, Fujita A, Tokumoto T, Fujimoto T (2006) Cytoplasmic lipid droplets are sites of convergence of proteasomal and autophagic degradation of apolipoprotein B. *Mol Biol Cell*, 17:2674–2683.
29. Thorne-Tjomsland G, *et al.* (2003) Characterization of lipid donor particles within ER/Golgi and post-ER degradation of VLDL assembly intermediates by an autophagy-like process in McA-RH7777 cells. *Mol Biol Cell* 14 (suppl):104a (abstr).
30. Tran K, *et al.* (2004) Attenuated hepatic assembly and secretion of VLDL by eicosapentaenoic acid treatment is associated with enhanced formation of autophagolysosomes. *Arterioscler Thromb Vasc Biol* 24:E57–E58 (abstr).
31. Klionsky DJ, Cuervo AM, Seglen PO (2007) Methods for monitoring autophagy from yeast to human. *Autophagy* 3:181–206.
32. Schroder M, Kaufman RJ (2005) The mammalian unfolded protein response. *Annu Rev Biochem* 74:739–789.
33. Pan M, Maitin V, Williams KJ, Fisher EA (2005) Regulation of hepatic assembly apolipoprotein B secretion by dietary polyunsaturated fatty acids involves apolipoprotein B aggregation and direct oxidative modification. *Arterioscler Thromb Vasc Biol* 25:E74 (abstr).
34. Takahashi M, *et al.* (2002) Fish oil feeding alters liver gene expressions to defend against PPARα activation and ROS production. *Am J Physiol Gastrointest Liver Physiol* 282:G338–G348.
35. Tran K, *et al.* (2002) Intracellular assembly of very low density lipoproteins containing apolipoprotein B100 in rat hepatoma McA-RH7777 cells. *J Biol Chem* 277:31187–31200.
36. Gusarova V, Brodsky JL, Fisher EA (2003) Apolipoprotein B100 exit from the endoplasmic reticulum (ER) is COPII-dependent, and its lipidation to very low density lipoprotein occurs post-ER. *J Biol Chem* 278:48051–48058.
37. Olofsson SO, Boren J (2005) Apolipoprotein B: A clinically important apolipoprotein which assembles atherogenic lipoproteins and promotes the development of atherosclerosis. *J Intern Med* 258:395–410.
38. Stefani M, Dobson CM (2003) Protein aggregation and aggregate toxicity: new insights into protein folding, misfolding diseases and biological evolution. *J Mol Med* 81:678–699.
39. Listenberger LL, Schaffer JE (2002) Mechanisms of lipoapoptosis: implications for human heart disease. *Trends Cardiovasc Med* 12:134–138.
40. Williams KJ, Fisher EA (2005) Oxidation, lipoproteins, and atherosclerosis: Which is wrong, the antioxidants or the theory? *Curr Opin Clin Nutr Metab Care* 8:139–146.
41. Williams KJ, Scalia R, Mazany KD, Rodrigueza WV, Lefer AM (2000) Rapid restoration of normal endothelial functions in genetically hyperlipidemic mice by a synthetic mediator of reverse lipid transport. *Arterioscler Thromb Vasc Biol* 20:1033–1039.
42. Bradley WA, Rhode MF, Gotto AM, Jr (1980) Studies on the primary structure of apolipoprotein B. *Ann NY Acad Sci* 348:87–103.
43. Khoo JC, Miller E, McLoughlin P, Steinberg D (1990) Prevention of low density lipoprotein aggregation by high density lipoprotein or apolipoprotein A-I. *J Lipid Res* 31:645–652.
44. Hoff HF, Whitaker TE, O'Neil J (1992) Oxidation of low density lipoprotein leads to particle aggregation and altered macrophage recognition. *J Biol Chem* 267:602–609.
45. Tabas I, Li Y, Brocia RW, Xu SW, Swenson TL, Williams KJ (1993) Lipoprotein lipase and sphingomyelinase synergistically enhance the association of atherogenic lipoproteins with smooth muscle cells and extracellular matrix. A possible mechanism for low density lipoprotein and lipoprotein(a) retention and macrophage foam cell formation. *J Biol Chem* 268:20419–20432.
46. Oorni K, Posio P, Ala-Korpela M, Jauhiainen M, Kovanen PT (2005) Sphingomyelinase induces aggregation and fusion of small very low-density lipoprotein and intermediate-density lipoprotein particles and increases their retention to human arterial proteoglycans. *Arterioscler Thromb Vasc Biol* 25:1678–1683.
47. Rosengren B, *et al.* (2006) Secretory phospholipase A2 group V: Lesion distribution, activation by arterial proteoglycans, and induction in aorta by a Western diet. *Arterioscler Thromb Vasc Biol* 26:1579–1585.
48. Wang H, Chen X, Fisher EA (1993) N-3 fatty acids stimulate intracellular degradation of apoprotein B in rat hepatocytes. *J Clin Invest* 91:1380–1389.
49. Borchardt RA, Davis RA (1987) Intrahepatic assembly of very low density lipoproteins. Rate of transport out of the endoplasmic reticulum determines rate of secretion. *J Biol Chem* 262:16394–16402.
50. Boren J, Rustaeus S, Olofsson SO (1994) Studies on the assembly of apolipoprotein B-100- and B-48-containing very low density lipoproteins in McA-RH7777 cells. *J Biol Chem* 269:25879–25888.
51. Glantz SA (2005) *Primer of Biostatistics* (McGraw Hill, New York).

Int. J. Cancer: **123,** 810–816 (2008)

TIP30 is associated with progression and metastasis of prostate cancer

Hui Zhang[1,2], Yifen Zhang[1,2], Hai Ou Duan[1,2], Sandra D. Kirley[2], Sharron X. Lin[2], W. Scott McDougal[2], Hua Xiao[3] and Chin-Lee Wu[1,2]*

[1]*Department of Pathology, Massachusetts General Hospital and Harvard Medical School, Boston, MA*
[2]*Department of Urology, Massachusetts General Hospital and Harvard Medical School, Boston, MA*
[3]*Department of Physiology and Pathology, Michigan State University, East Lansing, MI*

Tat-interacting protein 30 (TIP30), a transcriptional repressor for ERα-mediated transcription, possesses several characteristics of a tumor suppressor in certain human and mouse cells. It is reported that deletion of TIP30 gene preferentially increases tumorigenesis in the female knockout mice. Here, we analyzed TIP30 gene expression in the databases of several DNA microarray studies of human prostate cancer and show that TIP30 is specifically overexpressed in metastatic prostate cancers. We demonstrate that TIP30 nuclear expression is associated with prostate cancer progression and metastasis by immunohistochemical analysis in primary and metastatic prostate cancers. Consistent with these data, we also show that knockdown of TIP30 expression, through use of a short hairpin RNA-expressing plasmid, suppresses the cellular growth of PC3 and LNCaP prostate cancer cells. Ectopic overexpression of TIP30 stimulates metastatic potential of prostate cancer cells in an *in vitro* invasion assay, whereas knockdown of TIP30 inhibits the prostate cancer cells invasion. Finally, we demonstrate that ectopic overexpression of TIP30 enhances androgen receptor mediated transcription, whereas knockdown of TIP30 results in a decreased transcription activity. These data provide evidence that TIP30 plays a role in prostate cancer progression and that TIP30 overexpression may promote prostate cancer cell growth and metastasis.

Key words: TIP30; metastasis; progression; prostate cancer

Prostate cancer is the most common noncutaneous cancer of men in the United States. In 2007, 218,890 new cases and 27,050 deaths from prostate cancer were predicted in the USA (National Cancer Institute, http://www.cancer.gov/cancertopics/types/prostate). Its development proceeds through a series of defined states, including prostatic intraepithelial neoplasia, organ-confined prostate cancer, locally invasive cancer and metastatic cancer. The organ-confined prostate cancers are potentially curable with surgery and/or radiation. On the other hand, locally advanced tumors and metastatic prostate cancers are difficult to treat. The current treatment of metastatic prostate cancer is the use of androgen ablation because the growth of prostate cancer cells is dependent on the androgen hormone. However, this treatment sometime fails to cure the disease as the prostate cancer often becomes androgen-independent. It is believed that abnormal expression of components in the androgen-receptor-signaling pathway may contribute not only to the initiation but also to the progression of prostate cancers. Indeed, several transcriptional coactivators for the androgen receptor (AR) are implicated in the development and progression of prostate cancer.[1–3] However, the roles of AR coactivators in the promotion of prostate cancer metastasis are currently unknown.

A number of DNA microarray studies of gene expression in human prostate carcinomas reveal overexpression of a set of genes in metastatic prostate cancers, including hepsin[4,5] and the metastasis-associated gene 1 (MTA1).[6] Hepsin mRNA is upregulated in 90% of prostate tumors and exclusively expressed in tumor cells.[5] Overexpression of hepsin in prostate epithelium *in vivo* causes disorganization of the basement membrane.[7] In a mouse model of nonmetastasizing prostate cancer, hepsin overexpression also causes disorganization of the basement membrane and promotes primary prostate cancer progression and metastasis to liver, lung, and bone.[7] MTA1 is selectively overexpressed in metastatic prostate cancer compared with clinically localized prostate cancer and benign prostate tissue.[8]

TIP30 (Tat-interacting protein 30), also called CC3 or Htatip2, was identified as a transcriptional cofactor that enhances Tat-mediated transcription.[9] The TIP30/CC3 gene was independently identified by differential display analysis of mRNA from the highly metastatic human small cell lung carcinoma (SCLC) cell line when compared with the less metastatic SCLC cell lines.[10] Introduction of the TIP30/CC3 gene into a variant SCLC (v-SCLC) cell line that did not express the TIP30/CC3 gene resulted in a significant suppression of its metastatic potential. Intravenous delivery of the TIP30 gene to melanoma-bearing mice *via* a cationic liposome-DNA complex significantly reduced metastases.[11] TIP30 has been proposed to function as a metastasis suppressor *via* its ability to promote apoptosis and inhibit angiogenesis.[10,12–14] Consistent with this hypothesis, ectopic expression of TIP30 was found to elevate the expression of a subset of proapoptotic genes[14] and angiogenic inhibitors and to downregulate the expression of certain angiogenic stimulators.[13] Moreover, deletion of 1 or both alleles of *Tip30* resulted in spontaneous development of hepatocellular carcinoma and other tumors in mice.[15] Therefore, TIP30 played an inhibitory role in tumorigenesis in liver and lung cells. Unlike the finding in liver and lung cancer cells, a DNA microarray study on prostate cancer specimens suggested that TIP30 mRNA was overexpressed in prostate cancers.[5] Thus, we sought to further investigate whether TIP30 expression is associated with prostate cancer progression.

In this study, we characterized for the first time the role of TIP30 in prostate cancer. Expression microarray data were further analyzed to compare TIP30 gene expression in benign prostate tissues, clinically localized and metastatic prostate cancers. These analyses were validated with immunohistochemistry in human prostate cancer tissue samples. The effect of TIP30 on prostate cancer cell growth, metastatic/invasive potential and androgen receptor mediated transcription was analyzed. Our results indicate a stimulatory role of TIP30 in the growth, progression and metastasis of prostate cancer cells. Finally, the findings combined with previous studies on TIP30 provide an interesting model of the TIP30 with opposing effect on androgen/estrogen receptors and prostate/breast cancers.

Abbreviations: AR, androgen receptor; BPH, benign prostatic hyperplasia; KD, knockdown; Pca, prostate cancer; SCLC, small cell lung carcinoma; shRNA, short hairpin RNA; TGF-β, transforming growth factor-beta; TIP30, tat-interacting protein 30.

Grant sponsors: John and Clair Bertucci Foundation, T. J. Martell Foundation (C-LW); Grant sponsor: National Institute of Health Grants; Grant number: DK066110-01; Grant sponsor: American Cancer Society Grant; Grant number: RSG0216501GMC.

Yifen Zhang current address is: Department of Pathology, Nanjing Drum Tower Hospital, Nanjing University Medical School, Nanjing, Jiangsu, 210008, P.R. China.

***Correspondence to:** Departments of Pathology and Urology, Massachusetts General Hospital, Harvard Medical School, 55 Fruit Street, Boston, MA 02114, USA. Fax:+617-724-7803.
E-mail: cwu2@partners.org

Received 11 December 2007; Accepted after revision 12 March 2008
DOI 10.1002/ijc.23638
Published online 4 June 2008 in Wiley InterScience (www.interscience.wiley.com).

Material and methods

Data collection

The clone ID of TIP30 in the DNA microarray data of the study carried out by Dhanasekaran *et al*.[5] is 589751. The clone ID of TIP30 in the DNA microarray data of the study carried out by Holzbeierlein *et al*.[16] is 38824.

Immunohistochemistry

Affinity-purified anti-TIP30 rabbit polyclonal antibody was purified as described previously.[9] Tissue specimens were obtained from the pathology archive of Massachusetts General Hospital with permission given by the institutional human study committee. Formalin-fixed, paraffin-embedded tissue sections of radical prostatectomy specimens were stained with affinity-purified anti-TIP30 antisera at a 1:400 dilution using a microwave-enhanced avidin-biotin-staining ABC (Vector Labs, Burlingame, CA) method.[17,18] Negative control sections were immunostained under the same condition substituting preabsorbed antisera and preimmune rabbit antisera for primary antibodies. The stained slides were analyzed visually by 2 trained pathologists (CLW, YZ). Positive stain of TIP30 was defined as dark brown signals in the nuclei in the majority (>50%) of the tumor cells.

Generation of TIP30 overexpression and knockdown stable cell lines

Prostate cancer cell lines PC3 and LNCaP (ATCC, Manassas, VA) were grown in DMEM with 4.5 g/l of glucose and 10% FBS and used to generate TIP30 overexpressing or knockdown stable cell lines. To generate a stable TIP30 overexpressing PC3 cell line the pCIN4-TIP30 vector[14] was transfected into PC-3 cells using Lipofectamine 2000 (Invitrogen, Carlsbad, Ca). Transfected colonies were selected by growth in 1 mg/ml G418 (Meditech, Herndon, VA) and grown into stable clones then screened for TIP30 expression levels by Western blot. Control cells were made by transfecting the pCIN4 vector (Invitrogen) alone. To generate TIP30 knockdown PC3 and LNCaP cell lines the shRNA constructs were established using a pSilencer^{TM} 4.1-CMV neo kit (Ambion, Austin, TX). The shRNA target sequence of TIP30 gene, 5′-AATGGCTGGTTAGAAAGTTCTT-3′ (from No. 542 nt to No. 563 nt of TIP30 gene), was designed with a free software provided by Ambion. PC3 and LNCaP cells were transfected using Lipofectamine 2,000. After neomycin (1 mg/ml) selection, multiple clones were obtained and individual clones were picked and screened for reduced expression of TIP30 by Western blot analysis. The control p*Silencer* vector that expresses a scrambled control shRNA was also transfected into PC3 and LNCaP cells to generate stable control cell lines.

Determination of cell growth rate

The growth rates of PC3 control, PC3/TIP30/shRNA, LNCaP control, and LNCaP/TIP30/shRNA cells were determined by seeding 1×10^4 cells/well into 24-well tissue culture (TC) plate and counting the cells in quadruplicate for up to 11 days. The media was replaced every 3rd day. The growth rate for each cell line was determined from the exponential growth phase of the cells. Data are expressed as ± SD.

In vitro *invasion assay*

Invasion assays were performed using a BD BioCoat Matrigel invasion chamber according to the manufacture's instruction (BD Biosciences Discovery Labware, Bedford, MA). 1×10^4 cells in 500 μl of DMEM medium were seeded in the upper chamber, and 750 μl of DMEM medium with 10% FBS was added to lower chamber in 24-well TC plate. Cells were incubated at 37°C for 22 hr, then fixed and stained with the Diff-Quik stain set (Dade Behring, Newark, DE) according to the manufacture's instruction. Cells remaining on the underside of the membrane were counted. The experiments were run in triplicate and the results were averaged. Data was expressed as the percent of invasion through the Matrigel Matrix and membrane relative to the migration through the control membrane. The "Invasion Index" was expressed as the ratio of the percent invasion of a test cell over the percent invasion of a control cell.

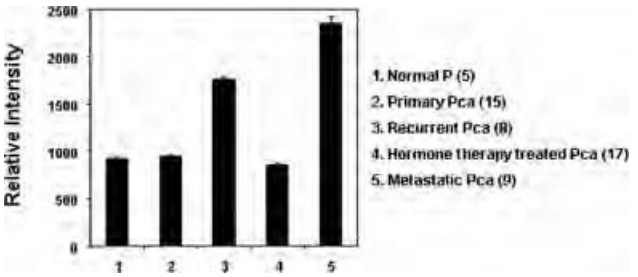

FIGURE 1 – TIP30 gene expression in normal and various prostate cancer (Pca) tissues. The RNA expression data were kindly provided by Dr. William L. Gerald. The relative intensity of TIP30 expression in the different tissues was plotted.

Transient transfection and androgen receptor mediated transcription assay

The AR expression vector was constructed by inserting its corresponding cDNA sequence into pcDNA3.1.[19] The luciferase reporter contained the androgen response element ahead of the E4 basal promoter and the luciferase gene.[19] Both plasmid constructs were kindly provided by Dr. Z. Wang from the MD Anderson Cancer Center (Houston, TX). The pCIN4-TIP30[14] expression vector was described previously. PC3 and LNCaP cells were transfected with plasmid DNA using the Lipofectamine 2,000 transfection reagent. Briefly, 3×10^5 cells were plated onto each well of 24-well plates ~24 hr before transfection and were transfected with 1 μg of total amount of DNA, which was adjusted with pCIN4. Transfections were conducted in Opti-MEM I Reduced Serum Medium (Invitrogen); 5 hr later, the medium was replaced with phenol-free DMEM plus charcoal-treated 10% FBS (Hyclone, Logan, UT) containing 10 nM R1881 (Perkin Elmer, Waltham, MA) for PC3 cells or 1 nM R1881 for LNCaP cells. Cells were cultured for another 48 hr and harvested for the dual luciferase assay (Promega, Madison, WI). In all experiments, a plasmid pRL-CMV for expressing *Renilla* Luciferase was used as a control for transfection efficiency, and activities of firefly and *Renilla* luciferase were measured with Promega Dual-Luciferase reporter system, normalized, and expressed as relative luciferase light units.

Results

TIP30 gene is overexpressed in metastatic and recurrent human prostate carcinomas

A number of DNA microarray studies have been performed to analyze the gene expression profile in prostate cancers.[4,5,6,16] Dhanasekaran *et al*. profiled and analyzed gene expression in normal prostate tissue, benign prostatic hyperplasia (BPH), localized and metastatic prostate cancer.[5] Their analysis indicated that gene expression of TIP30 was markedly upregulated in 8 out of 11 metastatic prostate cancers (73%), whereas expression of the TIP30 gene was unchanged in normal prostate tissue, BPH or localized prostate cancer. In the study published by Holzbeierlein *et al*., the gene expression in normal prostate tissue, primary prostate cancer, recurrent prostate cancer, hormone (goserelin and flutamide) treated primary prostate cancer, and metastatic prostate cancer was profiled.[16] We further analyzed the data and compared the specific expression patterns of TIP30 gene in these different prostate tissues. Consistent with the previous report, the gene expression of TIP30 was upregulated in recurrent and metastatic prostate cancers but not in primary or hormone therapy treated prostate cancers (Fig. 1). The analysis of TIP30 gene expression from the DNA microarray data indicated that the TIP30 gene was overexpressed in the metastatic prostate cancer.

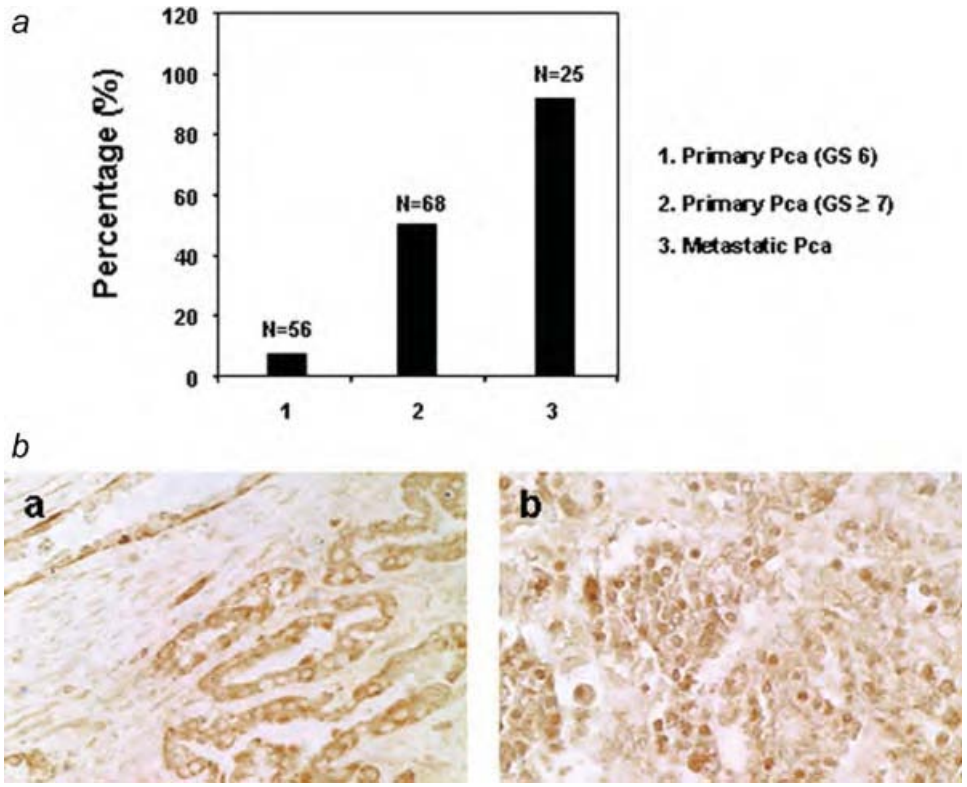

FIGURE 2 – (*a*) Immunohistochemical analysis of TIP30 expression in localized primary (Gleason score 6 cancer and Gleason score ≥7) and metastatic prostate cancers. *N* = sample number/group. The bar graph illustrates the percentage of specimens that demonstrated positive staining in each group. (*b*) Immunostaining of TIP30 in primary localized (panel a) and metastatic (panel b) prostate cancers. The upper left gland in Fig. 2(*b)* (panel a) is an adjacent normal prostatic acinar structure. The smaller cancer acinar glands are in the right bottom part of Fig. 2(*b*) (panel a). Metastatic prostate cancer cells in Fig. 2(*b)* (panel b) showed prominent TIP30 nuclear staining.

Immunohistological analysis of TIP30 expression in primary and metastatic prostate cancers

To study TIP30 expression in primary localized and metastatic prostate cancers, we performed immunohistochemical analysis using an affinity purified rabbit anti-TIP30 antibody on primary human prostate cancer radical prostatectomy specimens. We included Gleason score 6 cancer and higher grade (Gleason score 7 and above) cancers for this analysis which represent the vast majority of prostate cancers. Fifty-six localized Gleason score 6 prostate cancers, 68 localized higher-grade prostate cancers (Gleason scores 7 or above), and 25 metastatic prostate cancers were tested. TIP30 is expressed in the nuclei of basal cells and is negative in the nuclei of luminal cells of normal prostate acinar structures (Fig. 2*b* panel a, upper left). TIP30 expression was different among the different cancer groups (Fig. 2*a* and 2*b*). In localized Gleason score 6 cancers, 4 out of the 56 cases studied (7%) demonstrated positive TIP30 nuclear expression (Fig. 2*b* panel a, bottom right), compared to the adjacent normal luminal epithelium in prostate (Fig. 2*b* panel a, upper left). In the higher Gleason score (≥7) group of localized prostate cancers, 34 of the 68 cases (50%) showed positive nuclear staining. In the metastatic prostate cancers, 23 of the 25 cases (92%) showed positive nuclear staining (Fig. 2*a* and 2*b* panel b). To confirm the tissue section finding, when both endogenous and exogenous expressions of TIP30 were examined in cultured prostate cancer cells, the majority of TIP30 staining was found in the nucleus of both LNCaP and PC3 cells (data no shown). These data suggested that expression of TIP30 is associated with progression and metastasis of prostate cancer.

Regulation of prostate cancer cell growth by TIP30

To investigate the potential biological function of TIP30 in prostate cancer cells, we knocked down (KD) the TIP30 expression in both the PC3 and LNCaP cells by shRNA (short hairpin RNA) using pSilencer^{TM} 4.1-CMV neo kit and analyzed the expression levels and growth characteristics of the transfected cells compared with their parental controls. Multiple individual clones were established and we observed significantly reduced cell growth in all the clones with reduced TIP30 expression by TIP30 shRNA (data not shown). Figure 3*a* (panel a) illustrates the expression of TIP30 in the TIP30/shRNA compared with the control cells on a Western blot probed with antibody to TIP30. Figure 3*a* panel b showed that the TIP30 expression in PC3/TIP30/shRNA and LNCaP/TIP30/shRNA cells was significantly decreased. The densitometric analysis normalizing TIP30 protein relative to cellular actin protein showed that TIP30 expression in PC3/TIP30/shRNA cells and LNCaP/TIP30/shRNA cells decreased to 61% and 48% respectively when compared to their control cells.

To study the effect of TIP30 on cell proliferation, cell growth of PC3/TIP30/shRNA and LNCaP/TIP30/shRNA cells were determined and compared with that of their control cells (Fig. 3*b* and 3*c*). The doubling time of PC3/TIP30/shRNA cells was increased to 71 hr when compared with that of PC3 vector control cells (53 hr). The doubling time of LNCaP/TIP30/shRNA cells was increased to 65 hr when compared with that of LNCaP vector control cells (29 hr). These results indicated that TIP30 has a stimulatory role in cell growth of prostate cancer cells.

The effect of TIP30 expression on prostate cancer cell invasion

TIP30 expression is increased in higher grade and metastatic prostate cancer cells. We hypothesized that TIP30 may be associated with cell invasion of prostate cancer and tested this hypothesis in an *in vitro* system. A cell invasion test was performed using a Matrigel invasion chamber, an accepted assay correlated with

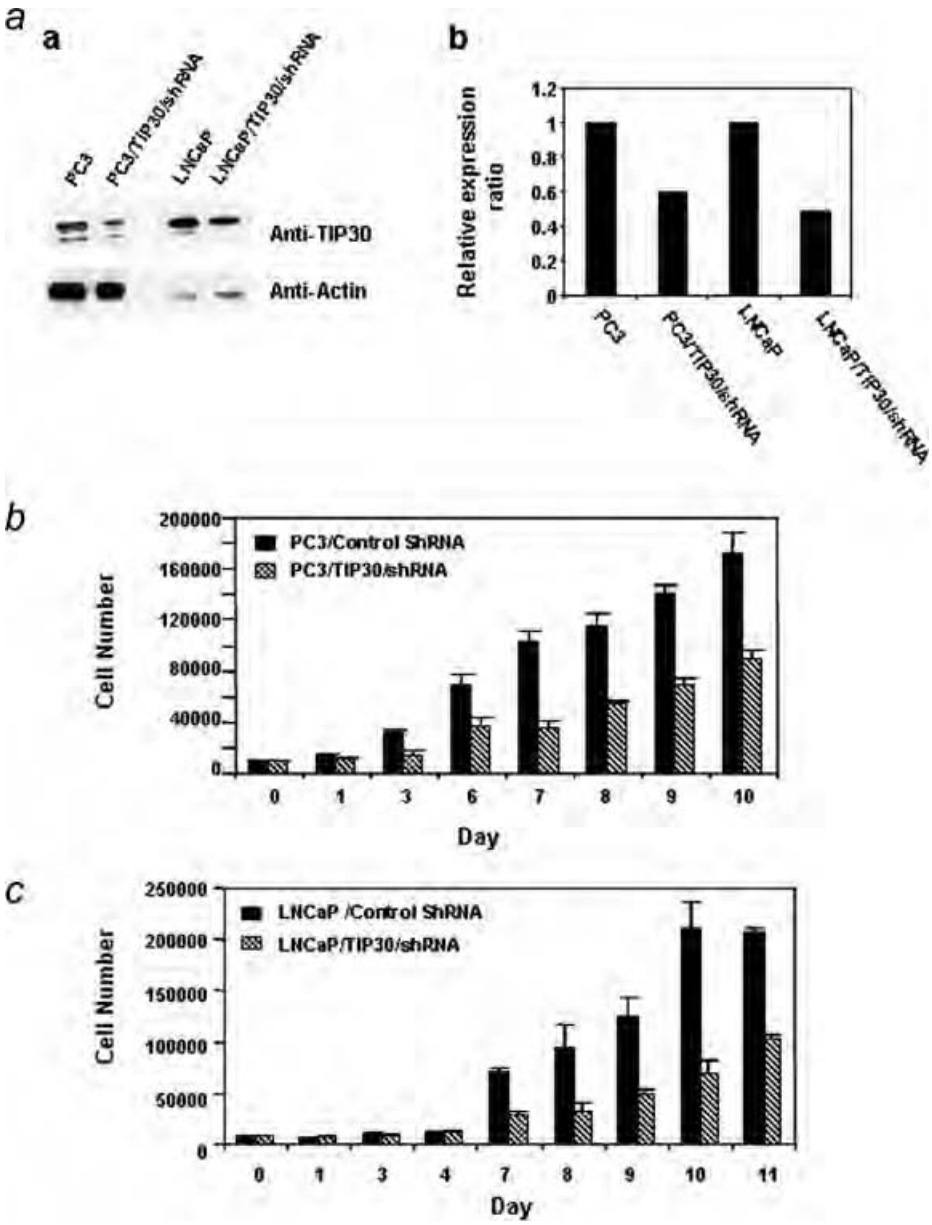

FIGURE 3 – [*a* (panel a)], Western blot analysis of TIP30 expression in TIP30 KD prostate cancer cells and their parent control cells containing vector alone. *a* (panel b), Densitometric analysis of immunoblot. Relative expression ratio of TIP30 expression to β-actin expression in TIP30 KD cells to that of their control cells. The relative expression ratio of TIP30 in control cells was given to 1. (*b*), Comparison of growth rate by cell number counting between PC3 control cells and PC3/TIP30/shRNA cells. (*c*), Comparison of growth rate between LNCaP control cells and LNCaP/TIP30/shRNA cells.

metastatic potential *in vitro*,[20,21] to study the effect of TIP30 on the metastasis of prostate cancer cells. The percent invasion of TIP30 KD cells was compared to that of their parent control cells (Fig. 4*a*). The invasion index of PC3/TIP30/shRNA cells was 70% to PC3 control cells and the invasion index of LNCaP/TIP30/shRNA cells was 41% to LNCaP control cells, indicating that knockdown of TIP30 in the cancer cells reduced the cell invasive ability. The TIP30 effect on invasion was also studied in prostate cancer cell line overexpressing TIP30. PC3 cells overexpressing TIP30 (PC3/TIP30) were established with transfection of pCIN4-TIP30[14] into PC3 cells. The control PC3 cell (PC3 vector) was also obtained by stably transfecting the pCIN4 vector alone. The overexpression of TIP30 in PC3 cell was confirmed by Western blot (Fig. 4*b* insert). The percent invasion of PC3/TIP30 cells was compared with PC3 vector cells. Two different concentrations of serum were used to test whether there was any alteration in cell motility. In the lower chamber filled with DMEM containing 10 or 5% FBS, the invasion index of PC3/TIP30 cells was 147 or 213% to PC3 vector control cells, respectively. These results indicated that overexpression of TIP30 in prostate cancer cells increased the cell invasion ability. Together, these observations indicated that TIP30 stimulates invasiveness and thus the metastatic potential of prostate cancer cells.

TIP30 enhances androgen receptor mediated transcription activity

The immunohistochemical study showed that TIP30 had a strong nuclear expression in higher-grade localized prostate cancers and in most metastatic prostate cancers, implying that TIP30 may play a role in nuclear regulation. TIP30 functions as a transcriptional regulator for ERα-mediated transcription.[22] Given the similarity between androgen and estrogen receptors and the role of androgen receptor (AR) in prostate cancer, we tested the possibility that TIP30 may regulate AR mediated transcription activity in prostate cancer. PC3 cells were transiently transfected with luciferase reporter driven human PSA promoter fragment[16] and pCDNA-AR, along with pCDNA-TIP30 expression vectors, as indicated in Figure 5*a*. Cells were grown in the presence of 1 nM DHT for 48 hr after transfection, and then harvested for dual

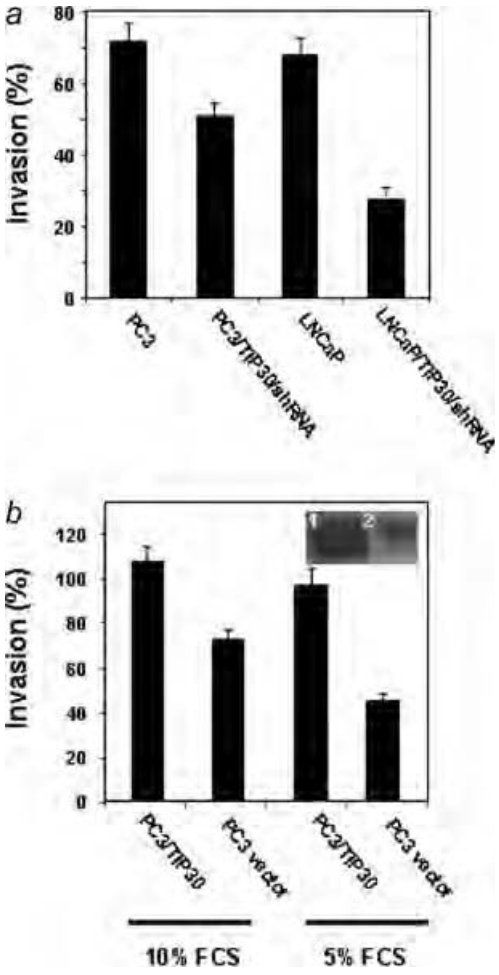

FIGURE 4 – (*a*), Comparison of the capacity of cell invasion between TIP30 KD cells and its control PC3 and LNCaP cells. Data were expressed as the percent invasion through the matrigel matrix and membrane relative to the migration through the control membrane. (*b*), Comparison of the capacity of cell invasion between PC3/TIP30 and control cells under different concentration of serum as chemoattractant. Western blot insert shows TIP30 expression in PC3/TIP30 (lane 1) and PC3 with expression vector (lane 2). The left side group represented the percent invasion of cells grown in the case of lower chamber with DMEM containing 10% FBS. The right side group represented the percent invasion of cells into the lower chamber having 5% FBS in DMEM.

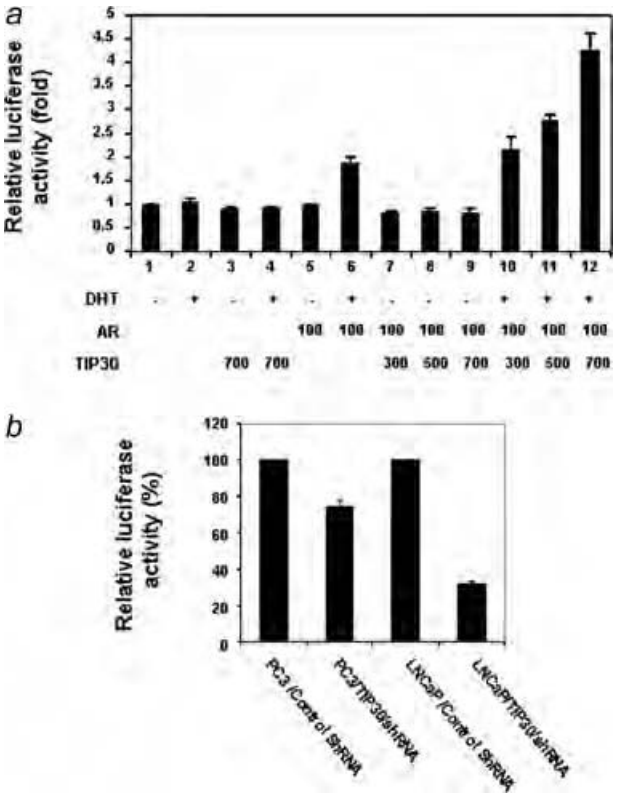

FIGURE 5 – (*a*), Effect of TIP30 overexpression on AR-mediated transcription. PC3 cells were transiently transfected with luciferase reporter driven by a 6.4 kb of human PSA promoter fragment and pCDNA-AR (100 ng), along with pCDNA-TIP30 expression vectors at 300, 500, and 700 ng. Cells were grown in the presence (+) or absence (−) of 1 nM DHT for 48 hr after transfection, and then harvested for dual luciferase activity assay. (*b*), Comparison of AR-mediated transcription activity of TIP30 KD cells with control cells. The stable shRNA expression cells were transfected with 200 ng of 4 × ARE-E4-luc report plasmid and pCDNA-AR. After transfection, cells were grown in the presence of 10 nM R1881 (for PC3 cells) or 1 nM R1881 (for LNCaP cells) and then harvested for luciferase activity assays. Relative luciferase activity represented the percentage of luciferase activity of TIP30 KD cells to that of the vector control cells.

luciferase activity assay. Along with increasing amount of co-transfected TIP30, the promoter activity increased correspondingly, and this effect was androgen-dependent. To confirm the TIP30 activation of AR-mediated transcription, we tested whether knockdown TIP30 expression would result in a decrease of AR-mediated transcription activity. As shown in Figure 5*b*, cells were transiently transfected with 4 × ARE-E4-luc reporter plasmid. In co-transfection with AR, the transcription activity of PC3/TIP30/shRNA cells was reduced to 75% of the PC3 control cells, while the relative transcription activity of LNCaP/TIP30/shRNA cells decreased to 32% of LNCaP control cells as expected. The luciferase reporter system in the study was not sensitive enough to determine the luciferase activity without the transfection of AR. *Renilla* Luciferase was used as a control for transfection efficiency and cell proliferation. Thus the effect of TIP30 on AR activation is not the result of TIP30 effect on cell growth. Together, these results indicate that TIP30 plays a role in AR-mediated transcription.

Discussion

The goal of this study was to understand the role of TIP30 in prostate cancer. A number of studies have been documented on gene expression profiles of human metastatic prostate cancer. TIP30 is one of the genes on the reported heatmaps that distinguish metastatic prostate cancer from clinically localized prostate cancer. In this study, we presented evidence that the expression of TIP30 protein in prostate epithelial cells was specifically upregulated in human higher grade prostate cancer (Gleason score ≥ 7) and metastatic prostate cancers. Inhibition of TIP30 by shRNA caused reduced proliferation of 2 tested prostate cancer cell lines. Overexpression of TIP30 led to an increased invasion capacity of these cell lines. Finally, we showed evidence that the effect of TIP30 in prostate cancer might be in part through its influence on AR transactivation of its target genes.

TIP30 was previously identified as a putative metastasis suppressor that inhibits metastasis of variant small cell lung carcinoma (v-SCLC).[10] Functional studies supported that overexpression of TIP30 in NIH3T3 and v-SCLC cells inhibited cell growth by predisposing cells to apoptosis.[13] The TIP30$^{-/-}$ mice have a high incidence of hepatocellular carcinoma, breast tumors and other tumors with metastases to multiple tissues, indicating that

TIP30 deficiency increases susceptibility to tumorigenesis.[15] Recent studies show that inhibition of TIP30 expression greatly enhanced the potential of breast cancer cell invasion,[23] and TIP30 deletion promotes proliferation of primary mammary epithelial cells (MEC) and results in rapid immortalization of MECs.[24] TIP30 overexpression represses ERα-mediated *c-myc* transcription, whereas TIP30 deficiency enhances *c-myc* transcription.[22] TIP30 mutations not only loss the function of tumor suppression but also gain functions such as acceleration of tumorigenesis by altering the expression of the *N-cadherin* gene.[25] Those could be the mechanisms by which TIP30 influences tumorigenesis. Interestingly, throughout this study, we found that alteration of TIP30 had effects on both LNCaP and PC3 prostate cancer cells. However, when examining cell growth and invasion, much greater effects were consistently observed in androgen-sensitive LNCaP cells when compared with that in androgen-insensitive PC3 cells (Figs. 3 and 4). When reduction of AR-mediated transcription activity was measured, the relative transcription activity was reduced to 32% in LNCaP cells but only reduced to 75% in PC3 cells. Although our data indicate the potential involvement of TIP30 in AR-mediated pathways to regulate prostate cancer metastasis, our data did not exclude the possibility of TIP30 regulating other pathways to promote prostate cancer metastasis. In fact the expression of TIP30 in androgen insensitive PC3 cells suggests that signals other than AR-mediated pathway may interact with TIP30 to facilitate prostate cancer progression. More work is needed to further elucidate these interactions. Our findings of the role of TIP30 in the development of prostate cancer showed that TIP30 promoted the growth of prostate cancer cells, enhanced metastatic potential of prostate cancer cells, and enhanced AR-mediated transcription, suggesting that TIP30 has a distinct role in prostate tissue and plays a bifunctional role in tumorigenesis.

A few genes that play bifunctional tumor suppressor/oncogene role in tumorigenesis have been reported. Transforming growth factor-beta (TGF-β) through its unique transmembrane receptor serine-threonine kinases, posses both tumor suppressor and oncogenic activities, playing a complex role in carcinogenesis.[26] Tumor cells often escape from the antiproliferative effects of TGF-β by mutational inactivation or dysregulated expression of components in its signaling pathway. Decreased receptor function and altered ratios of the TGF-β type I and type II receptors found in many tumor cells compromise the tumor suppressor activities of TGF-β and enable its oncogenic functions. The complex of TGF-β and endoglin, an important modulator of TGF-β1 signaling, was elevated markedly in breast cancer patients who developed metastasis and/or died of the disease.[27] On the other hand, overexpression of betaglycan, an endoglin homologue, in human breast cancer MCF-7 cells increased the autocrine activity of TGF-β and reduced the clonogenicity of the cells in soft agar.[28] In another human breast cancer line, MDA-MB-231, it resulted in reduced tumorigenicity *in vivo*.[29] Furthermore, estrogens are believed to play critical role in prostate cancer progression and estrogen receptor-β was shown to be regulated in a reversible and cancer stage-specific fashion. Its expressions decreased during localized prostate cancer progression (from lower to higher grade) but increased in metastatic prostate cancer.[30,31]

Our data suggested that TIP30 may play a stimulatory role in the pathways of cancer cell progression and metastasis in prostate cells that is different from lung and breast cells, raising an interest to identify the downstream target genes of TIP30 in this disease. Previous studies have shown that several DNA-repair and metastasis-related genes (including RPA70, NM23-H2 and RAP) in small lung carcinoma cells are induced by TIP30[14] and *c-myc* expression in breast cells is inhibited by TIP30.[22] Here, we demonstrated that TIP30 in prostate cancer cells enhanced AR-mediated transcription activity, which is required for prostate cancer development and progression. It is tempting to speculate that TIP30 might act as a coactivator in AR-mediated transcription. Nevertheless, the validation of the speculation requires further experimentation. Unraveling the role of TIP30 might provide novel connections between regulatory networks for prostate cancer metastasis and help the development of new strategy for therapeutic treatment for human cancer.

Acknowledgements

The authors would like to acknowledge Drs. William L. Gerald for kindly providing the TIP30 gene expression data of their DNA microarray profiles.

References

1. Chua SS, Ma Z, Ngan E, Tsai SY. Cdc25B as a steroid receptor coactivator. Vitam Horm 2004;68:231–56.
2. Gregory CW, He B, Johnson RT, Ford OH, Mohler JL, French FS, Wilson EM. A mechanism for androgen receptor-mediated prostate cancer recurrence after androgen deprivation therapy. Cancer Res 2001;61:4315–19.
3. Agoulnik IU, Vaid A, Bingman WE, III, Erdeme H, Frolov A, Smith CL, Ayala G, Ittmann MM, Weigel NL. Role of SRC-1 in the promotion of prostate cancer cell growth and tumor progression. Cancer Res 2005;65:7959–67.
4. Luo J, Duggan DJ, Chen Y, Sauvageot J, Ewing CM, Bittner ML, Trent JM, Isaacs WB. Human prostate cancer and benign prostatic hyperplasia: molecular dissection by gene expression profiling. Cancer Res 2001;61:4683–8.
5. Dhanasekaran SM, Barrette TR, Ghosh D, Shah R, Varambally S, Kurachi K, Pienta KJ, Rubin MA, Chinnaiyan AM. Delineation of prognostic biomarkers in prostate cancer. Nature 2001;412:822–6.
6. Varambally S, Dhanasekaran SM, Zhou M, Barrette TR, Kumar-Sinha C, Sanda MG, Ghosh D, Pienta KJ, Sewalt RG, Otte AP, Rubin MA, Chinnaiyan AM. The polycomb group protein EZH2 is involved in progression of prostate cancer. Nature 2002;419:624–9.
7. Klezovitch O, Chevillet J, Mirosevich J, Roberts RL, Matusik RJ, Vasioukhin V. Hepsin promotes prostate cancer progression and metastasis. Cancer Cell 2002;6:185–95.
8. Hofer MD, Kuefer R, Varambally S, Li H, Ma J, Shapiro GI, Gschwend JE, Hautmann RE, Sanda MG, Giehl K, Menke A, Chinnaiyan AM, et al. The role of metastasis-associated protein 1 in prostate cancer progression. Cancer Res 2004;64:825–9.
9. Xiao H, Tao Y, Greenblatt J, Roeder RG. A cofactor. TIP30, specifically enhances. HIV-1 Tat-activated transcription. Proc Natl Acad Sci USA 1998;95:2146–51.
10. Shtivelman E. A link between metastasis and resistance to apoptosis of variant small cell lung carcinoma. Oncogene 1997;14:2167–73.
11. Liu Y, Thor A, Shtivelman E, Cao Y, Tu G, Heath TD, Debs RJ. Systemic gene delivery expands the repertoire of effective antiangiogenic agents. J Biol Chem 1999;274:13338–44.
12. NicAmhlaoibh R, Shtivelman E. Metastasis suppressor CC3 inhibits angiogenic properties of tumor cells in vitro. Oncogene 2001;20:270–5.
13. Whitman S, Wang X, Shalaby R, Shtivelman E. Alternatively spliced products CC3 and TC3 have opposing effects on apoptosis. Mol Cell Biol 2000;20:583–93.
14. Xiao H, Palhan V, Yang Y, Roeder RG. TIP30 has an intrinsic kinase activity required for up-regulation of a subset of apoptotic genes. Embo J 2000;19:956–63.
15. Ito M, Jiang C, Krumm K, Zhang X, Pecha J, Zhao J, Guo Y, Roeder RG, Xiao H. TIP30 deficiency increases susceptibility to tumorigenesis. Cancer Res 2003;63:8763–7.
16. Holzbeierlein J, Lal P, LaTulippe E, Smith A, Satagopan J, Zhang L, Ryan C, Smith S, Scher H, Scardino P, Reuter V, Gerald WL. Gene expression analysis of human prostate carcinoma during hormonal therapy identifies androgen-responsive genes and mechanisms of therapy resistance. Am J Pathol 2004;164:217–27.
17. Hsu SM, Raine L, Fanger H. Use of avidin-biotin-peroxidase complex (ABC) in immunoperoxidase techniques: a comparison between ABC and unlabeled antibody (PAP) procedures. J Histochem Cytochem 1981;29:577–80.
18. Yang WI, Zukerberg LR, Motokura T, Arnold A, Harris NL. Cyclin D1 (Bcl-1. PRAD1) protein expression in low-grade. B-cell lymphomas and reactive hyperplasia. Am J Pathol 1994;145:86–96.
19. Hosohata K, Li P, Hosohata Y, Qin J, Roeder RG, Wang Z. Purification and identification of a novel complex which is involved in androgen receptor-dependent transcription. Mol Cell Biol 2003;23:7019–29.
20. Repesh LA. A new in vitro assay for quantitating tumor cell invasion. Invasion. Metastasis 1989;9:192–208.
21. Robinson VL, Kauffman EC, Sokoloff MH, Rinker-Schaeffer CW. The basic biology of metastasis. Cancer Treat Res 2004;118:1–21.

22. Jiang C, Ito M, Piening V, Bruck K, Roeder RG, Xiao H. TIP30 interacts with an estrogen receptor α-interacting coactivator CIA and regulates c-myc transcription. J Biol Chem 2004;279:27781–9.
23. Zhao J, Ni H, Ma Y, Dong L, Dai J, Zhao F, Yan X, Lu B, Xu H, Guo Y. TIP30/CC3 expression in breast carcinoma: relation to metastasis, clinicopathologic parameters, and P53 expression. Hum Pathol 2007; 38:293–8.
24. Pecha J, Ankrapp D, Jiang C, Tang W, Hoshino I, Bruck K, Wagner KU, Xiao H. Deletion of Tip30 leads to rapid immortalization of murine mammary epithelial cells and ductal hyperplasia in the mammary gland. Oncogene 2007;26:7423–31.
25. Jiang C, Pecha J, Hoshino I, Ankrapp D, Xiao H. TIP30 mutant derived from hepatocellular carcinoma specimens promotes growth of HepG2 cells through up-regulation of *N*-cadherin. Cancer Res 2007; 67:3574–82.
26. de Caestecker MP, Piek E, Roberts AB. Role of transforming growth factor-beta signaling in cancer. J Natl Cancer Inst 2000;92: 1388–402.
27. Kumar S, Ghellal A, Li C, Byrne G, Haboubi N, Wang JM, Bundred N. Breast carcinoma: vascular density determined using CD105 antibody correlates with tumor prognosis. Cancer Res 1999;59:856–61.
28. Chen C, Wang XF, Sun L. Expression of transforming growth factor beta (TGF-β) type III receptor restores autocrine TGFbeta1 activity in human breast cancer MCF-7 cells. J Biol Chem 1997;272:12862–7.
29. Sun L, Chen C. Expression of transforming growth factor beta type III receptor suppresses tumorigenicity of human breast cancer MDA-MB-231 cells. J Biol Chem 1997;272:25367–72.
30. Leav I, Lau KM, Adams JY, McNeal JE, Taplin ME, Wang J, Singh H, Ho SM. Comparative studies of the estrogen receptors beta and alpha and the androgen receptor in normal human prostate glands, dysplasia, and in primary and metastatic carcinoma. Am J Pathol 2001;159:79–92.
31. Zhu X, Leav I, Leung YK, Wu M, Liu Q, Gao Y, McNeal JE, Ho SM. Dynamic regulation of estrogen receptor-beta expression by DNA methylation during prostate cancer development and metastasis. Am J Pathol 2004;164:1883–6.